SANDIA REPORT

SAND2016-XXXX Unlimited Release Printed May 2016

EMES Characterization

Robert A. Salazar, Megan E. Daily, Joseph M. Rudys, John L. Brown

Prepared by Sandia National Laboratories Albuquerque, New Mexico 87185 and Livermore, California 94550

Sandia National Laboratories is a multi-mission laboratory managed and operated by Sandia Corporation, a wholly owned subsidiary of Lockheed Martin Corporation, for the U.S. Department of Energy's National Nuclear Security Administration under contract DE-AC04-94AL85000.

Approved for public release; further dissemination unlimited.



Issued by Sandia National Laboratories, operated for the United States Department of Energy by Sandia Corporation.

NOTICE: This report was prepared as an account of work sponsored by an agency of the United States Government. Neither the United States Government, nor any agency thereof, nor any of their employees, nor any of their contractors, subcontractors, or their employees, make any warranty, express or implied, or assume any legal liability or responsibility for the accuracy, completeness, or usefulness of any information, apparatus, product, or process disclosed, or represent that its use would not infringe privately owned rights. Reference herein to any specific commercial product, process, or service by trade name, trademark, manufacturer, or otherwise, does not necessarily constitute or imply its endorsement, recommendation, or favoring by the United States Government, any agency thereof, or any of their contractors or subcontractors. The views and opinions expressed herein do not necessarily state or reflect those of the United States Government, any agency thereof, or any of their contractors.

Printed in the United States of America. This report has been reproduced directly from the best available copy.

Available to DOE and DOE contractors from

U.S. Department of Energy Office of Scientific and Technical Information P.O. Box 62 Oak Ridge, TN 37831

Telephone: (865) 576-8401 Facsimile: (865) 576-5728 E-Mail: reports@osti.gov

Online ordering: http://www.osti.gov/scitech

Available to the public from

U.S. Department of Commerce National Technical Information Service 5301 Shawnee Rd Alexandria, VA 22312

Telephone: (800) 553-6847 Facsimile: (703) 605-6900 E-Mail: orders@ntis.gov

Online order: http://www.ntis.gov/search



SAND2016-XXXX Unlimited Release Printed May 2016

EMES Characterization

Robert A. Salazar, Megan E. Daily, Joseph M. Rudys, John L. Brown

Electrical Sciences & Experiments, Dept. 1353
Sandia National Laboratories
P.O. Box 5800
Albuquerque, New Mexico 87185-MS1152

Abstract

The Electromagnetic Environment Simulator (EMES) is a large transverse electromagnetic (TEM) cell that propagates an ostensibly uniform, planar electromagnetic wave illuminating a test object with RF energy within a working volume. The characterization presented in this report uses measurements from three electric field components spanning a frequency range between 100 kHz and 220 MHz. This report provides guidance for using these results to predict measurement uncertainty for experiments conducted in EMES.

Weapons Systems Engineering Assessment Technology (WSEAT) commissioned this effort to provide support to Nuclear Weapons qualification in accordance with Realize Product Sub System (RPSS). Motivation for this effort stems from four qualification programs: B61 LEP, W88 ALT370, W80-4 LEP, and the Mk21 fuze program.

ACKNOWLEDGMENTS

The authors would like to acknowledge support received in executing these measurements and performing a reviewer of this document. Reviewers for formatting and technical content include: Clare Amann, Mike Dinallo, Matt Halligan, Mark Jursich, and Steve Glover.

CONTENTS

1.	Introduction	8
2.	Description of EMES	10
3.	Test Objectives	14
4. 4.1 4.2		16
5.	Results	20
6.	Recommended Application of This Data	48
7.	References.	50
Distribu	ıtion	51

FIGURES

Figure 1.	EMES Cutaway Diagram	10
Figure 2.	EMES Working Volume Dimensions (x is the radial dimension)	12
Figure 3.	Planes that cut the sample space	14
Figure 4.	Instrumentation Setup	16
Figure 5.	EMES Floor Probe Location Map	17
Figure 6.	Propagation of RF energy into EMES	17
Figure 7.	ETS E-Field Probe	18
Figure 8.	Injected and Reflected Power	19
Figure 9.	All results for Radial = 0 plane	21
Figure 10	Reference Probe	23
	Cross Polarization	
Figure 13	Radial Plane = 1	26
	Radial Plane = 0	
Figure 14	Radial Plane = 1, 2 m x 2 m area	27
_	Radial Plane = 2	
_	Radial Plane = -1 , 2 m x 2 m area	
	Radial Plane = -1	
	Vertical Plane = -1, 2 m x 2 m area	
_	Vertical Plane = 1	
_	200 kHz Results, Radial = 0 m Plane	
_	8 MHz Results, Radial = 0 m Plane	
_	. 15 MHz Results, Radial = 0 m Plane	
_	47 MHz Results, Radial = 0 m Plane	
_	63 MHz Results, Radial = 0 m Plane	
_	0.2 MHz Results, Horizontal = 0 m Plane	
_	8 MHz Results, Horizontal = 0 m Plane	
_	. 15 MHz Results, Horizontal = 0 m Plane	
_	47 MHz Results, Horizontal = 0 m Plane	
_	63 MHz Results Horizontal = 0 m Plane	
	H-field Measurement at 0.2 MHz	
	. H-field Measurement at 7 MHz	
-	. H-field Measurement at 8 MHz	
_	Direction of Propagation	
-	H-field Measurement at 15 MHz	
	H-field Measurement at 47 MHz	
Figure 36	. H-field Measurement at 63 MHz	46

NOMENCLATURE

dB decibel

DOE Department of Energy

DUT Device under test

E-field Electric Field

EM Electromagnetic

EMES Electromagnetic Environment Simulator

EMP Electromagnetic Pulse

EMR Electromagnetic Radiation

GTEM Gigahertz Transverse Electromagnetic

M-field Magnetic Field

NW Nuclear Weapons

RF Radio Frequency

RPSS Realize Product Sub System

SNL Sandia National Laboratories

TEM Transverse Electromagnetic

V/m Volts per meter

W Watt

1. INTRODUCTION

EMES simulates a free field electromagnetic environment to test the behavior or coupling factors of a test object subjected to free field electromagnetic energy. EMES is a tool Sandia uses to perform electromagnetic measurements on objects for different customers. Several customers from the nuclear weapons community have a need to obtain information about objects to meet electromagnetic qualification. Sandia employs the Realize Product Sub System (RPSS) to qualify Nuclear Weapons. RPSS requires that all processes follow strict guidelines ensuring contractual requirements and implementation of best practices, integration of operational requirements into mission planning and execution, and provide consistency in the delivery of high quality product. RPSS requires a good understanding of any tool used to characterize nuclear weapons. The results obtained from the tool must define and document uncertainties of the component for qualification. Concerns about this aging facility, degradation of RF absorbers, and need to meet RPSS requirements motivated the characterization of the uniformity of the electric field within its working volume of EMES.

E-field characterization measurements collected in February 2016 provide a measure of the uniformity of the electromagnetic field within the EMES working volume. The sensors used for this characterization were three axis probes that captured the magnitude of each polarization of the electric field. The number of test points provides sufficient spatial resolution to address field non-uniformities in the test volume. This report describes the processes and techniques used to acquire this information. In addition, this report provides guidance for using this information for qualification of nuclear weapons.

2. DESCRIPTION OF EMES

EMES is a large transverse electromagnetic (TEM) cell that propagates a uniform planar electromagnetic wave through a working volume. This facility occupies the purpose-built building 871 in Tech Area 1, Sandia New Mexico. Figure 1 shows a cutaway diagram of the building. RF energy enters EMES from the transition feed located in the control room. EMES combines the basic elements of a parallel plate transmission line and an anechoic chamber into a rectangular coaxial transmission line with a matched termination load. The facility is a bounded wave transmission line allowing broadband Electromagnetic Radiation (EMR) testing, Electromagnetic Pulse (EMP) testing of systems, subsystems, and components in a single facility. Reference (Seely & Thomas, 1978) reports EMES performance measured in 1978.

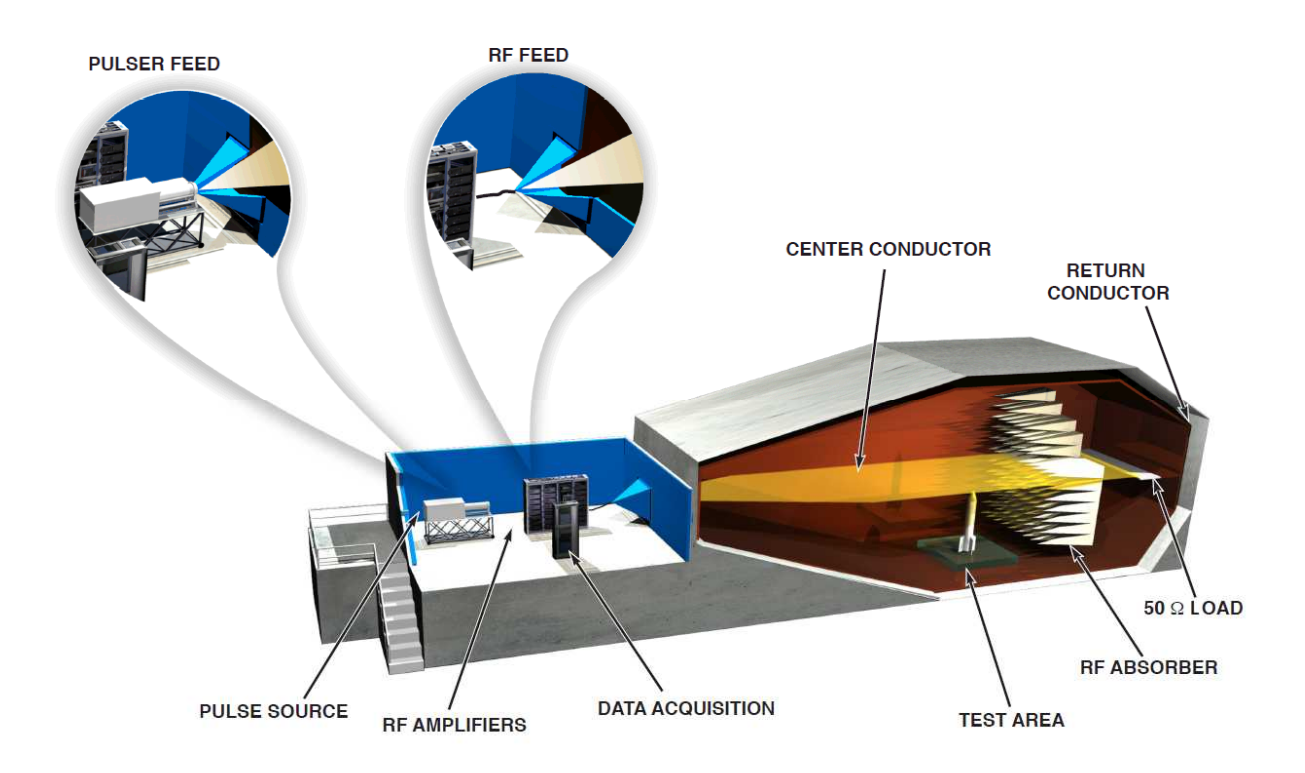


Figure 1. EMES Cutaway Diagram

A source drives the input to EMES. In the case of EMR, a signal generator drives an amplifier. The amplifier drives EMES (feed) input and develops the power and energy necessary to

stimulate the test object. Originating at the EMES input, a vertical electric field propagates between the center conductor and the bottom conductor through the working volume and terminates into a matched load. A resistor network provides the termination for lower frequencies. RF absorbers provide termination for higher frequencies. For a detailed discussion of the theory of operation of EMES refer to (Varnado, 1975, SAND1975-0412) and (Salazar, January 2016). Refer to (Crawford, Generation of Standard EM Fields Using TEM Transmission Cells, November 1974), (Crawford & Workman, Using a TEM cell for EMC measurements of electronic equipment, July 1981), and (Malaric, Bartolic, & Modlic, 2000) for more information about general TEM cells and GTEM cells.

Figure 2 shows a diagram of the working volume of EMES. The working volume is defined as the useful testing volume of 4 m by 8 m by 2 m centered between the center conductor and the floor (vertical dimension), between the ramp and RF absorbers (radial dimension), and between the sidewalls (horizontal dimension). Unlike GTEM cells, EMES has a well-defined operational boundary.

The bottom figure shows a side view of the working space. The center conductor (septum) is the top of the working space. The depth of the working space is 4 meters, defined by the edge of the sloping floor from the source and the edge of the RF absorbing cones. The top figure shows the working width of EMES, which is 8 meters. The volume defined in Figure 2 is the volume characterized in this report. This report also provides results of a smaller volume. EMES stimulus of smaller object has less field variation than field variation experienced by a larger object.

Due to material performance of any absorbing chamber similar to EMES, the injected power is not completely absorbed. The consequence is reflections cause constructive and destructive interference producing variations in field strength from point-to-point in the entire structure, not just the working volume. Further, point-to-point field strength changes with frequency. At a single point, field strength may change as much as 20 dB over the full test range of frequencies with constant injected power. The results section of this report describes this behavior.

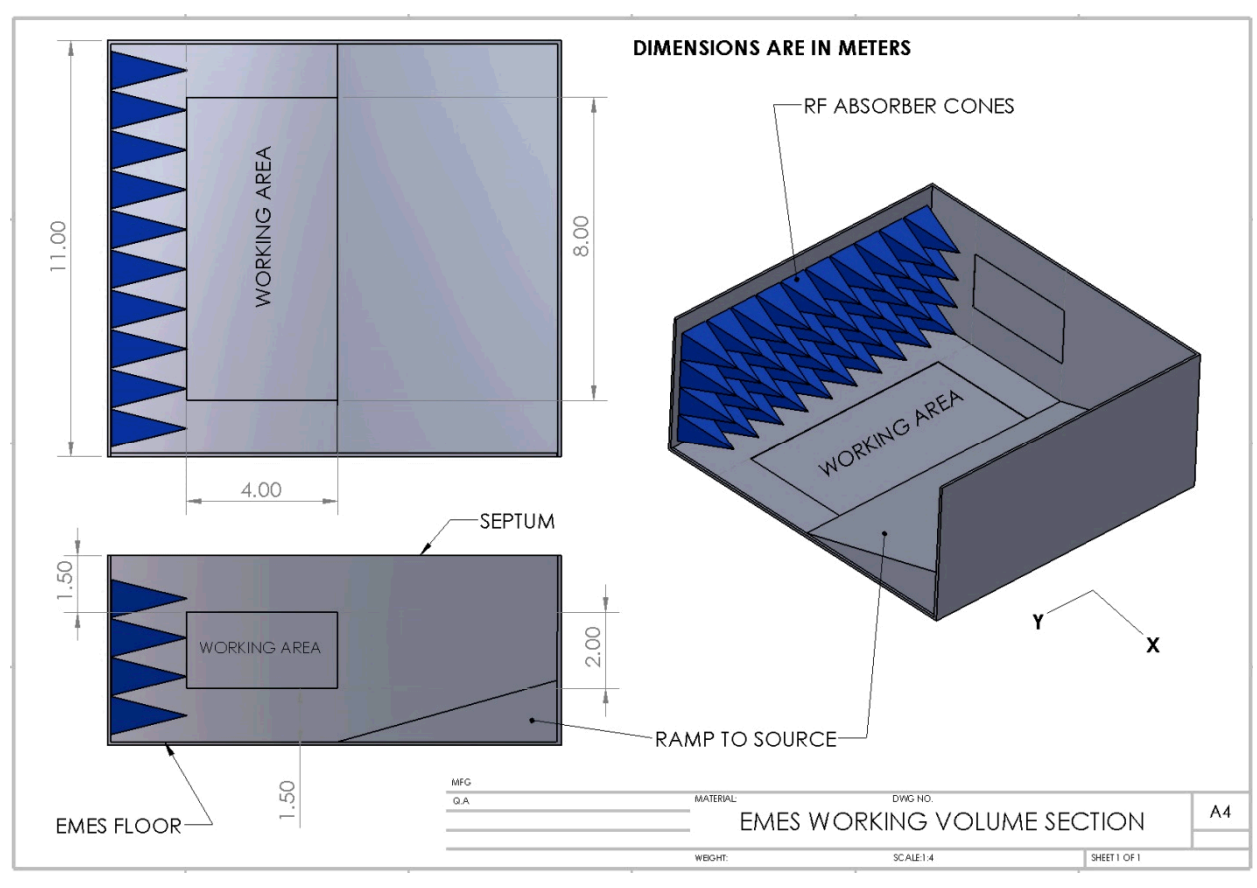


Figure 2. EMES Working Volume Dimensions (x is the radial dimension)

3. TEST OBJECTIVES

The primary objective of this effort was to evaluate EMES ability to produce a free field environment and quantify the quality of the field environment by evaluating the uniformity and purity of the electric field in EMES. EMES was empty during the test; hence, EMES is the sole source of reflections and standing wave structure and hence the uniformity and purity results. The 'results section' of this report defines uniformity and purity. A secondary objective was to determine the repeatability of the E-field generated by a constant input power. A third objective was to measure the absolute E-field generated in EMES as a function of drive power. This effort accomplished all three objectives by measuring the electric field at numerous locations within EMES and evaluating the point-to-point field-strength variance.

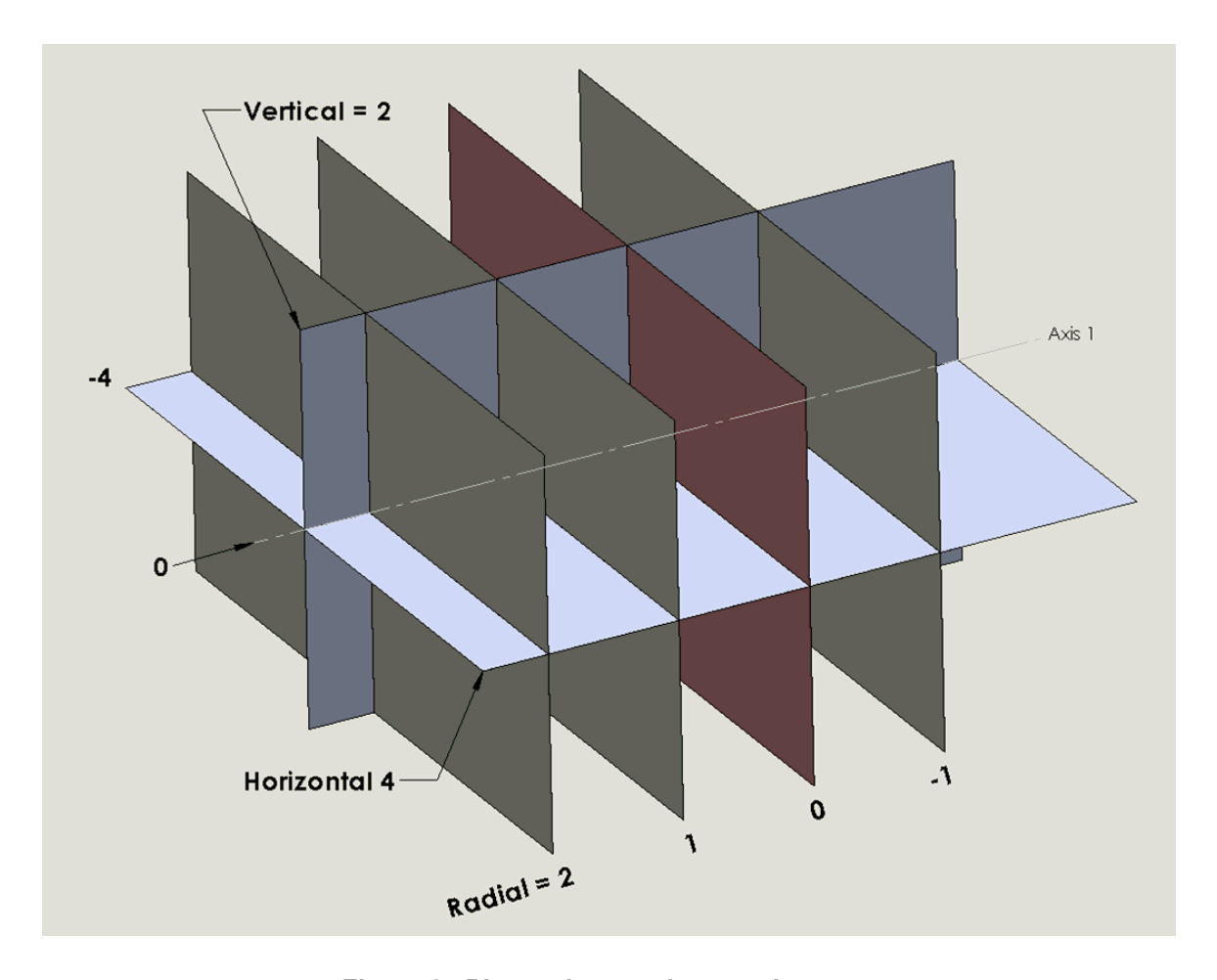


Figure 3. Planes that cut the sample space

4. TEST SETUP

4.1 Instrumentation

Figure 4 shows the instrument setup for this effort. The main components include a 500-watt amplifier and ETS tri-axial electric field probes. The amplifier provided a drive of 400-watt into EMES developing a nominal 35 V/m field measured by the ETS probes. The ETS tri-axial electric field probes are commercially available probes. Sandia Primary Standards Laboratory calibrated all instruments used to collect data for this effort.

A LabVIEWTM program ran the controller, setting the operational frequency and power levels of the RF energy entering EMES. The program recorded forward power, reverse power, test frequency, and all four ETS probe data into a single file for each test location.

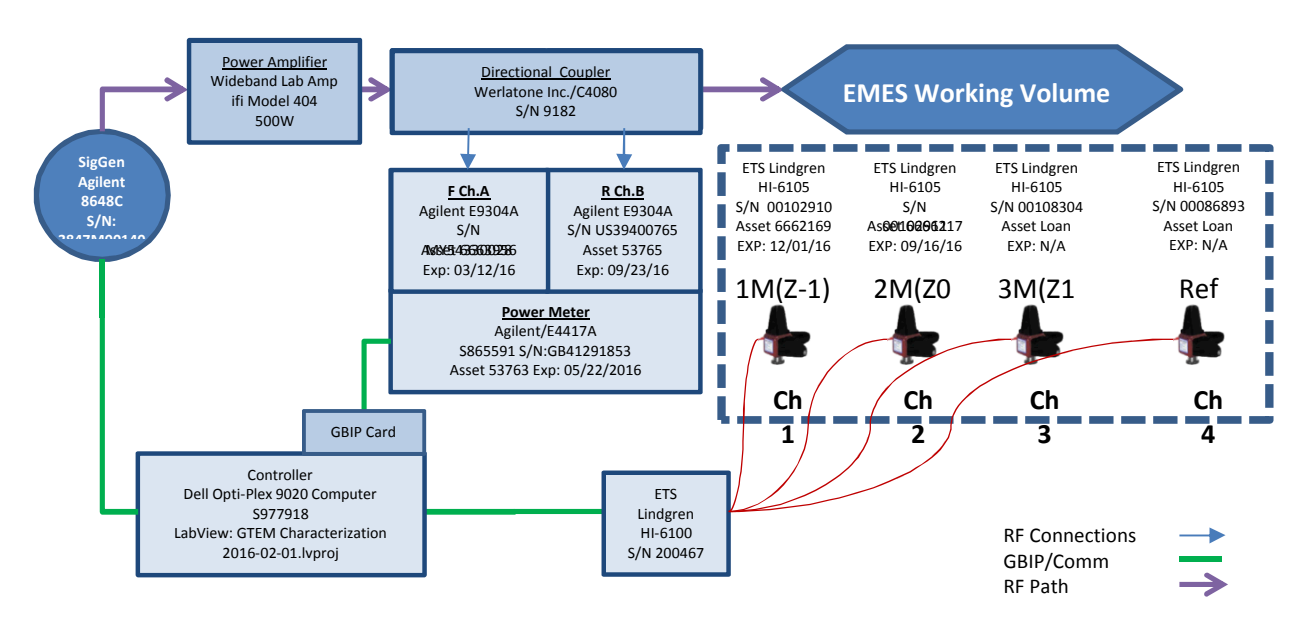


Figure 4. Instrumentation Setup

4.2 Probe Layout

Figure 5 shows the footprint of probe locations. The values shown on the perimeter are distances in meters from the center of the working volume. The numbers in the center identify the probe positions. Figure 6 shows a view of the anechoic cones inside EMES from the perspective of the source looking at the test object with the cones in the background. The primary component of the electric field is expected to be in the vertical direction shown in this figure. ETS probes occupy heights -1, 0, and 1 meter as measured from the center between the floor and septum. The coordinate system and labels are as follows: vertical refers to the case where the electric field is vertical; horizontal is the case where the electric field is orthogonal to the vertical field and the length of EMES; and radial is orthogonal to both the vertical and horizontal directions

				С		С		С		С		С		С		С		
				0		0		0		0		0		0		0		
				1		1		1		1		1		1		1		
				u		u		u		u		u		u		u		
				m		m		m		m		m		m		m		
				n		n		n		n		n		n		n		
				-3		-2		-1		0		1		2		3		
										cones								
		-4	-3.5	-3	-2.5	-2	-1.5	-1	-0.5	0	0.5	1	1.5	2	2.5	3	3.5	4
	-1.5									23								
row -1	-1	56	54	52	50	48	46	44	42	21	41	43	45	47	49	51	53	55
	-0.5									19								
row 0	0	16	14	12	10	8	6	4	2	1	3	5	7	9	11	13	15	17
	0.5									18								
row 1	1	40	38	36	34	32	30	28	26	20	25	27	29	31	33	35	37	39
	1.5									22								
row 2	2	72	70	68	66	64	62	60	58	24	57	59	61	63	65	67	69	71
										source								

Figure 5. EMES Floor Probe Location Map

representing the direction along the centerline of EMES. The data presented in subsequent sections use slices of these data representing planes of propagation. For example, in the slice labeled Radial = 0, all the values in the row containing 1 through 17 represents one plane. Four radial planes were measured (2, 1, 0, -1). This effort measured one column in ½-meter increments down the center of EMES; these results are present later in this document. Location 55 served as a reference point for all the measurements. A single ETS probe occupied height - 1 m at this location and the LabViewTM program recorded the E-field for every test except the measurement for location 55. In addition to E-field measurements, one set of \dot{B} measurements at radial = 0 and a height = 0 m recorded the magnetic field along a single line. During magnetic field measurements, the E-field reference probe at location 55 continued to measure E-field. The results section of this this report gives a comparison of E-field to H-field results.

The three tri-axial ETS electric field probes measured the three vector components of the electrical field. A fiberglass test stand held the three probes in place. The data from the probes transmitted via a fiber optical system to the system controller.

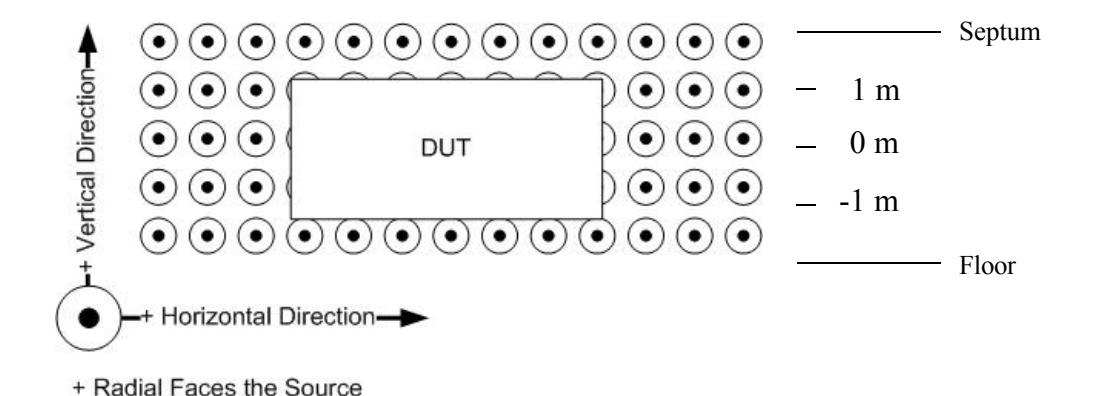


Figure 6. Propagation of RF energy into EMES

Figure 7 shows an ETS HI-6105 E-Field Probe used to measure E-field. These probes have three orthogonal elements each measuring the magnitude of the radial, horizontal, and vertical components. The probes occupied three heights in each position illustrated in Figure 5. The E-field settled to a steady-state condition at each frequency before the controller obtained each measurement.

The graphics, presented later in this report, plot the results of each plane for a single frequency. Therefore, each plot comprises measurements for the same number of files as points represented in the plot. Since there is measurement-to-measurement variation in amplifier output, the algorithm normalized the data to the square root of net power delivered for each measurement. The graphs show the normalized E-field values.



Figure 7. ETS E-Field Probe

Figure 8 shows RF power levels used during EMES characterization. The intended power was 56 dBm ±4 dB. The actual power was between 53 and 58 dBm. The top two graphs show forward and reverse power into EMES. In the second row, the left graph is a representation of net power. The right graph shows the drive level. At the highest return loss, reflected power was -6 dB or 25% of the injected power. The bottom row shows the reflection coefficient and the VSWR over the frequency range of the test. The highest reflection occurred at about 10 MHz. This is the transition frequency where the resistive load effectiveness diminishes and the RF cones begin to absorb RF energy. (Salazar, January 2016) gives details of EMES theory of operation.

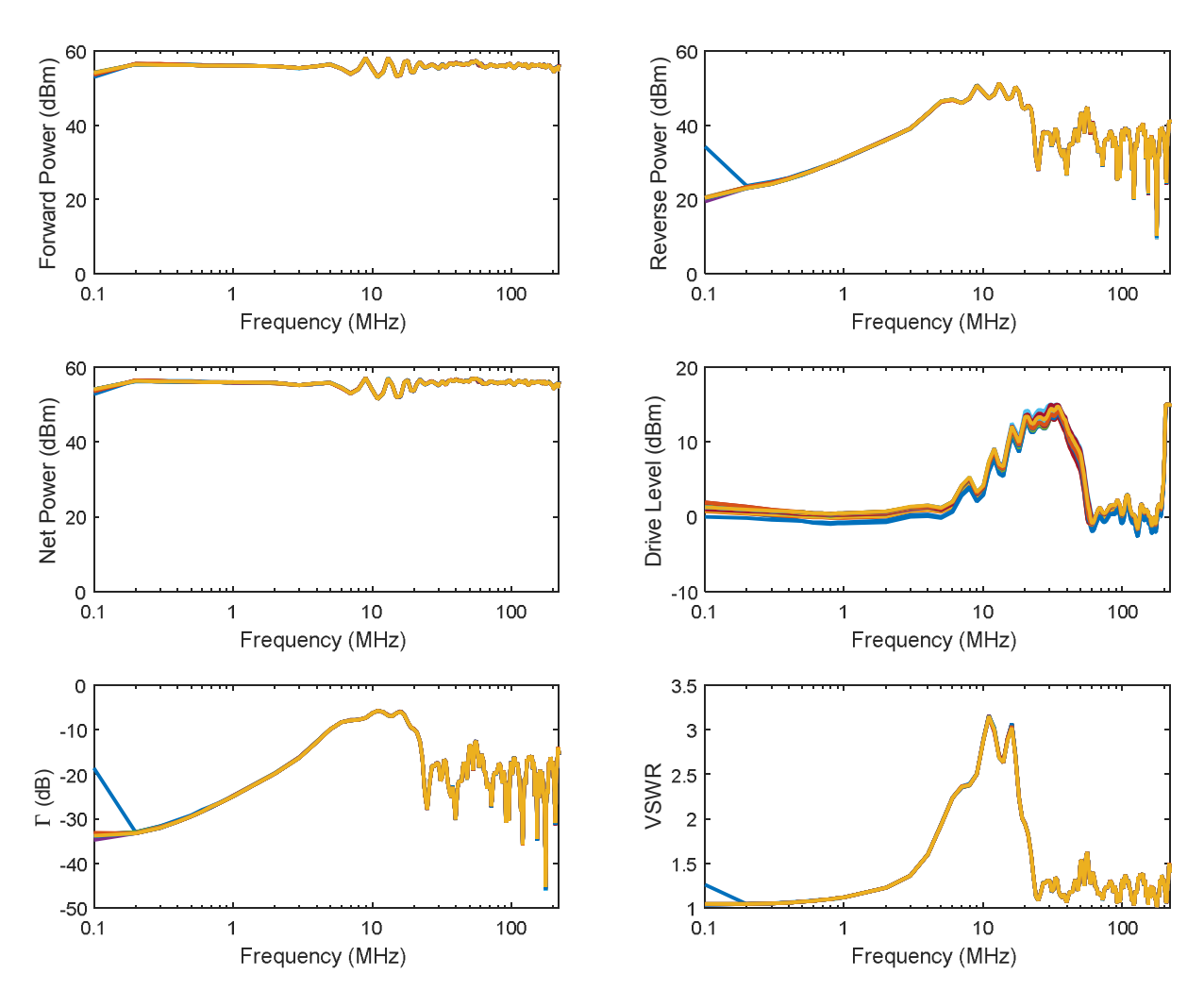


Figure 8. Injected and Reflected Power

5. RESULTS

Test results show EMES creates a well-behaved field distribution up to about 30 MHz. Above 30 MHz, reflections in EMES create field variations influencing uniformity and purity. Although the fields above 30 MHz do not adhere to a structure with good termination behavior, they are relatively uniform and variations in field strength are sufficiently for some test programs.

Measurement runs occurred at a single location over the entire frequency range. Uniformity results are displayed at several locations for a single frequency. Presenting the data in this manner, from different measurement setups, makes it likely each point experienced a different injection power due to normal equipment performance. To produce consistent results from different measurement sets, we normalized each data set to the square root of input power. For this reason, the parameter plotted in the uniformity graphics is in units of $\left(\frac{V}{m\sqrt{W}}\right)$. In addition to this normalization, a reference probe at a fixed location measured three-axis field strength during every measurement. The reference probe was an ETS three-axis probe; therefore, the probe measured field strength in all three axes. The reference probe results appear later in this document and show little E-field variation at the reference point for all testing.

The following presents details of data from Row 0 defined by points 1 through 17. This row of data defines a plane orthogonal to the intended direction of propagate in EMES. Also presented is a summary of all the data collected.

Figure 9 shows nine graphs, summarizing the E-field measured in EMES. These plots are comprised of the 17 points that represent the Radial = 0 plane. Figure 5 shows the 17 probe locations. The top row of Figure 9 shows all three E-field (vertical, radial, and horizontal) measurements for the full frequency range. The vertical component dominated the energy propagating in EMES below 40 MHz, which is EMES intended operation. The red dotted horizontal line denotes the lower boundary of the electric field probe calibration. Any measurement below the red dotted line is not reliable. The top center graph between 10 MHz and 20 MHz shows E-field variations that are a consequence of reflections from EMES termination. Reflections from the walls also contribute to the mode structure making a more significant contribution above 50 MHz. Independent of the reflections within the EMES volume, reflections at the feed also contribute to E-field variations. Reference (Salazar, January 2016) reports a TDR measurement that indicates the EMES feed exhibits a lower reflection value than suggested by these results.

The second row of graphs shows net power corrected results. All graphs in the center column represent the vertical field component, which is the intended primary component. Although field strength varied location-to-location and frequency-to-frequency, net power compensated data provides a valid representation of EMES E-field across the volume of EMES for all frequencies.

The bottom row of graphs shows the measurement standard deviation normalized to mean electric field. The E-field for the vertical component has very low variation while the radial and horizontal component variations are large compared to their mean values.

Using Figure 6 as a reference, the plots shown in this section of the report illustrate the response for measurements along the radial dimension.

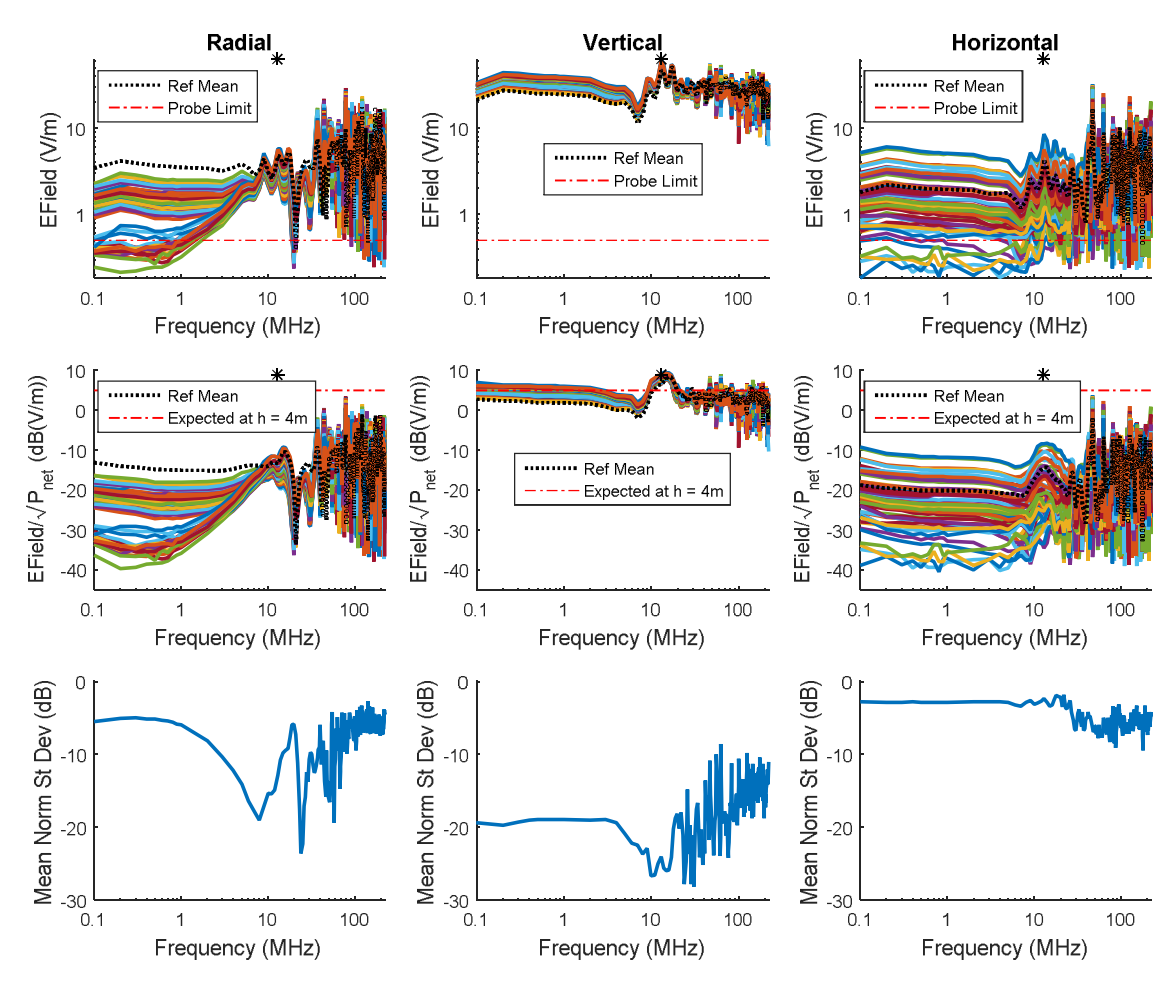


Figure 9. All results for Radial = 0 plane

To understand the net power correction, refer to Equation 1 that computes the expected E-field. Assuming power is 400 watts, Z_o is 50 Ω , and height is 4 m, the expected E-field is 35 V/m, well within the safe operating region of the probes. Most vertical measurements were close to 35 V/m. The asterisk in each graph marks the frequency and highest E-field (61.7 V/m) for all measurements. Equation 2 computes E-field normalized by net power and is used to generate the second row of graphs. Converting results from a linear to a log scale the expected normalized E-Field is $4.9 \, dB \left(\frac{V}{m \sqrt{watt}} \right)$.

$$E\left(\frac{V}{m}\right) = \frac{\sqrt{P(W) * Z_o(\Omega)}}{h(m)}$$

Equation 1. E-field for a given power and center conductor height

$$\frac{E\left(\frac{V}{m}\right)}{\sqrt{P(W)}} = \frac{\sqrt{Z_o(\Omega)}}{h(m)}$$

Equation 2. E-field normalized to square root of net power

Figure 10 shows reference probe results. The reference probe occupied location (-1, 4, -1) as drawn in the location map in Figure 5. The graphs clearly show that the injected power into EMES measurement-to-measurement was consistent. The reader can see the differences between measurements were very small. In most cases, the mean normalized standard variation was less than -30 dB.

Figure 11 shows the cross polarization components in EMES compared to the primary vertical E-field. The cross-polarized components are Radial, Horizontal, and $(\sqrt{Radial^2 + Horizontal^2})$. The graphs clearly show good polarization below approximately 30 MHz. Above 40 MHz, the radial and horizontal components are roughly the same magnitude as the vertical component. The radial component is particularly high above 70 MHz, with some frequencies showing a higher radial component than vertical component. In order to compare these results more directly within the EMC community using IEC 61000-4-20, a different representation of results following later in this section.

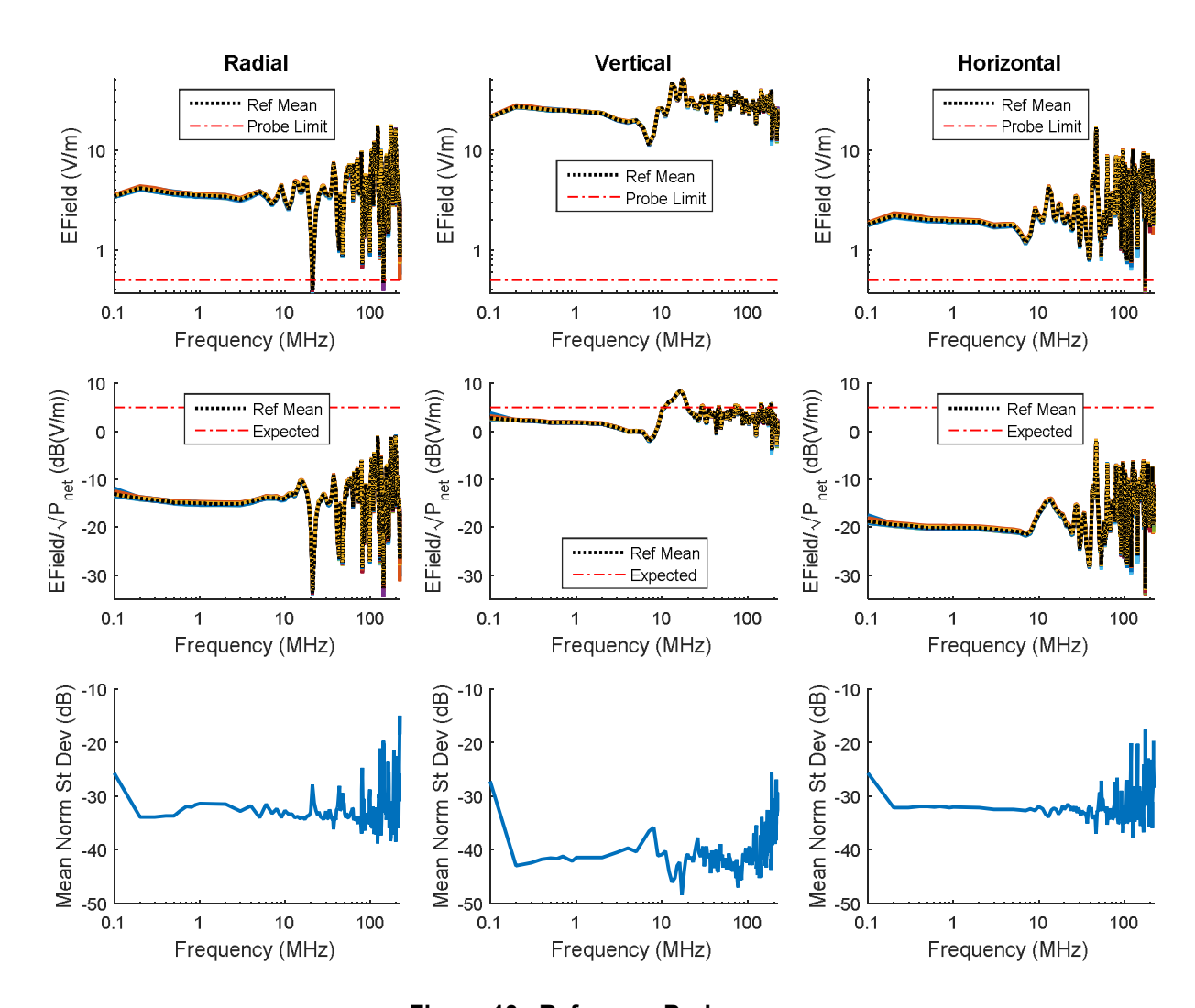


Figure 10. Reference Probe

Above 40 MHz, EMES behaves more as a resonating cavity than a transmission line. The E-field components are a sum of all the reflected energy in EMES. Measurements results in this report are from the stimulus of a continuous wave source. Hence, EMES standing waves greatly affected the E-field distribution. It is worth noting that the radial field in the direction of intended propagation should have zero field strength for TEM propagation. However, once energy enters EMES it reflects off several surfaces with some loss at each reflection. The energy from reflections eventually drops to a level that eliminates their contribution to the measured E-Field.

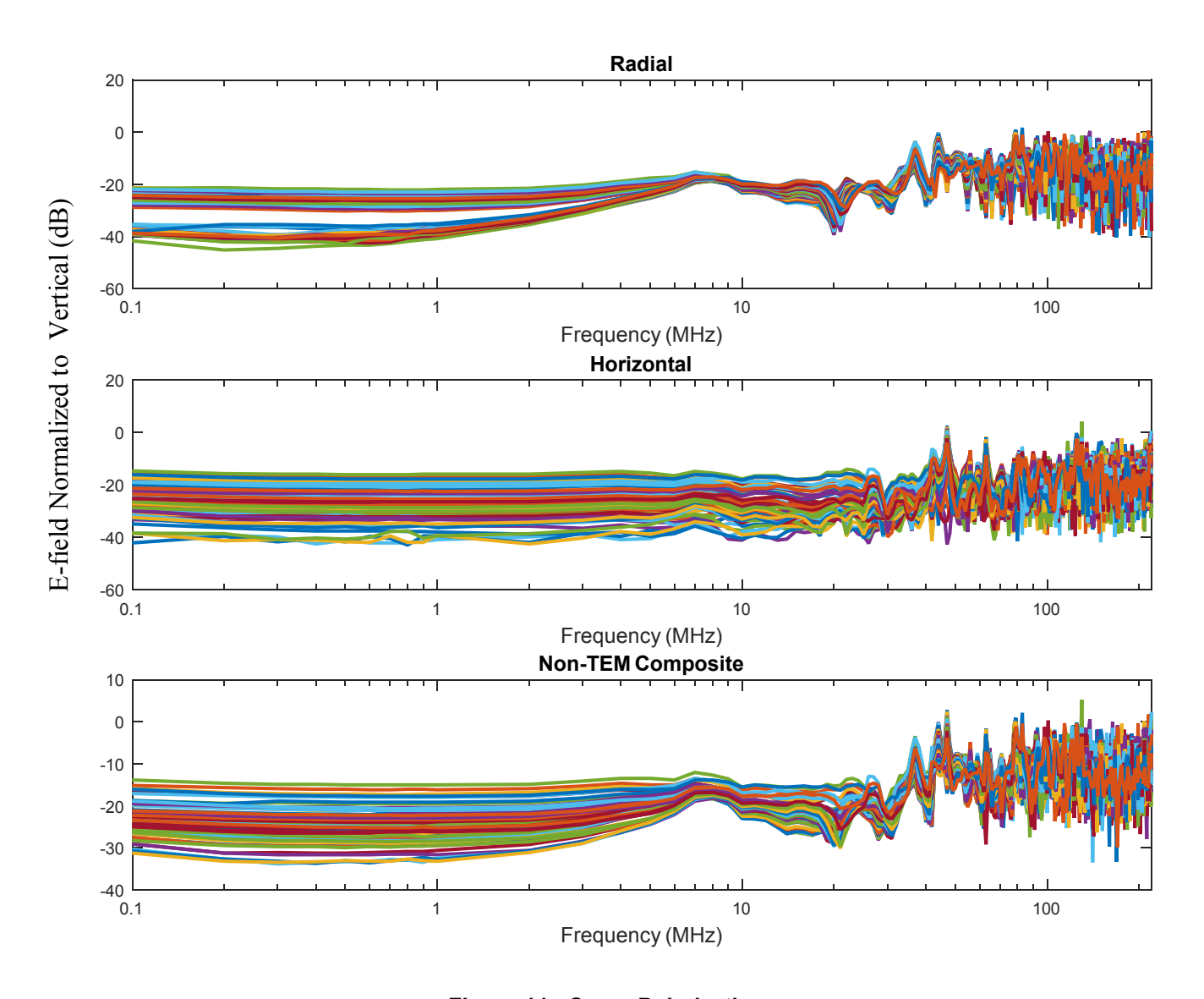


Figure 11. Cross Polarization

Figure 12 shows field uniformity and purity plots for a 2 m by 8 m area in the plane where Radial = 0. Figure 13 shows field uniformity and purity plots for a 2 m by 8 m area in the plane where Radial = 1 m. The field uniformity plot represents data calculated using Equation 3. Field

uniformity represents E_{max} (the maximum vertical E-field) for all measured points in the plane, divided by E_{min} (the minimum vertical E-field) for all measured points in the plane. Per IEC 61000-4-20 using 75% of the data collected, 95% of the uniformity data should not exceed +6 dB (with no data exceeding +10 dB).

The standard defines purity as the primary component (vertical) compared to the secondary components (horizontal and radial) computed using Equation 4. Per IEC 61000-4-20 using 75% of the data collected, 95% of the purity data should not be less than 6 dB (with no results less than 2 dB).

Uniformity =
$$20 \log_{10} \left(\frac{E_{max}}{E_{min}} \right)$$

Equation 3. Field Uniformity Calculation

Purity =
$$20 \log_{10} \left(\frac{E_Z}{E_{\text{secondary}}} \right)$$

Equation 4. Field Purity Calculation

Comparing Figure 12 and Figure 13, the uniformity is better at location radial = 0 than radial = 1; however, the purity is about the same for both locations. Since most EUTs will not fill the entire working area of EMES, the uniformity and purity of a smaller volume is important to understand. For this purpose, we considered a smaller area (2 m by 2 m). The equivalent plane for the radial = 0 m plane will still be at the radial = 0 location, but will now only consist of points between -1 m and +1 m in both the vertical and horizontal dimensions.

Comparing Figure 13 and Figure 14, it is clear that the uniformity and purity improves with a smaller area. Therefore, smaller objects will experience a better uniformity and a purer environment than a larger object; consequently, the user must consider the size and location of the test object in order to determine the uncertainty seen during testing.

Figure 14 though Figure 19 show results for a smaller area 2 m by 2 m. The earlier plots show results from a 2 m by 4 m area.

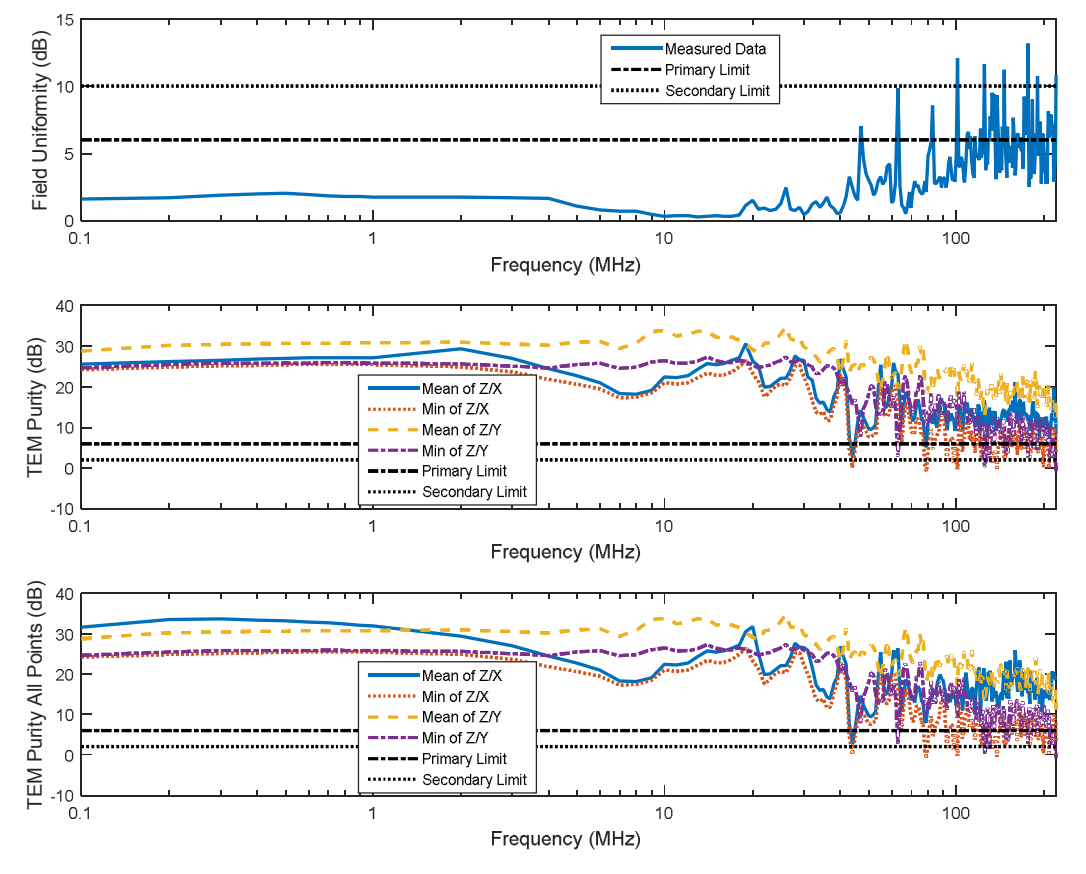


Figure 13. Radial Plane = 0
Uniformity Specification < 6 dB; Purity Specification > 6 dB

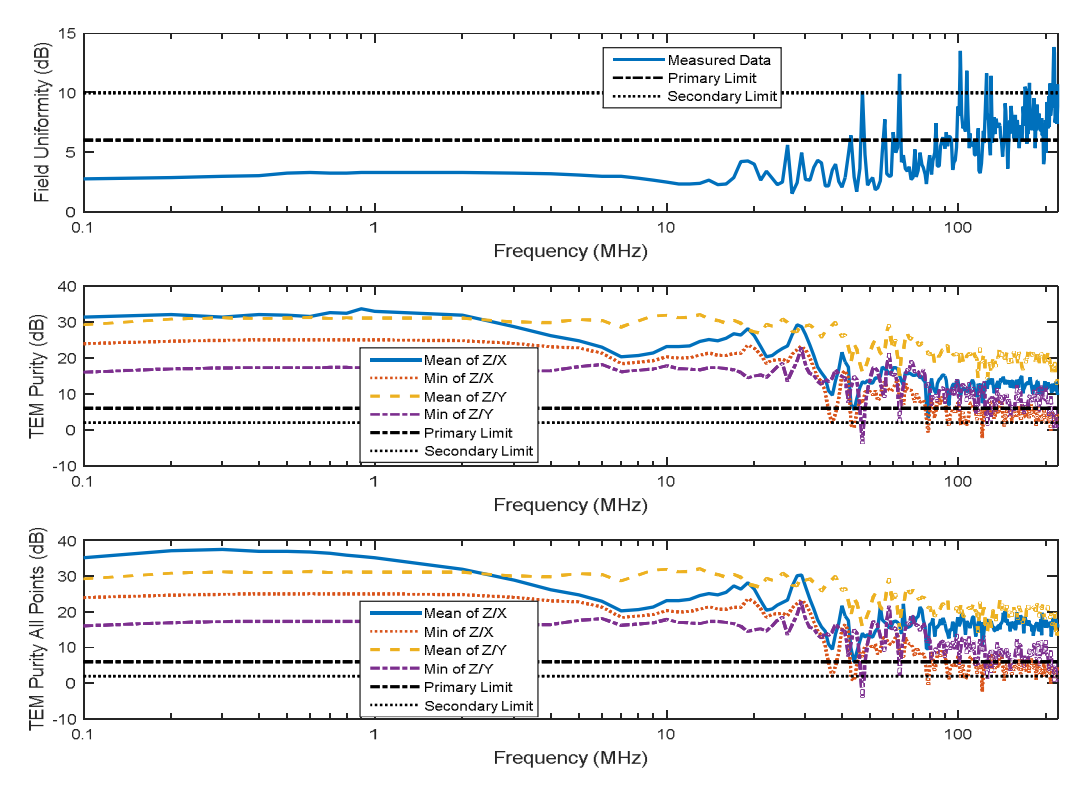


Figure 12. Radial Plane = 1
Uniformity Specification < 6 dB; Purity Specification > 6 dB

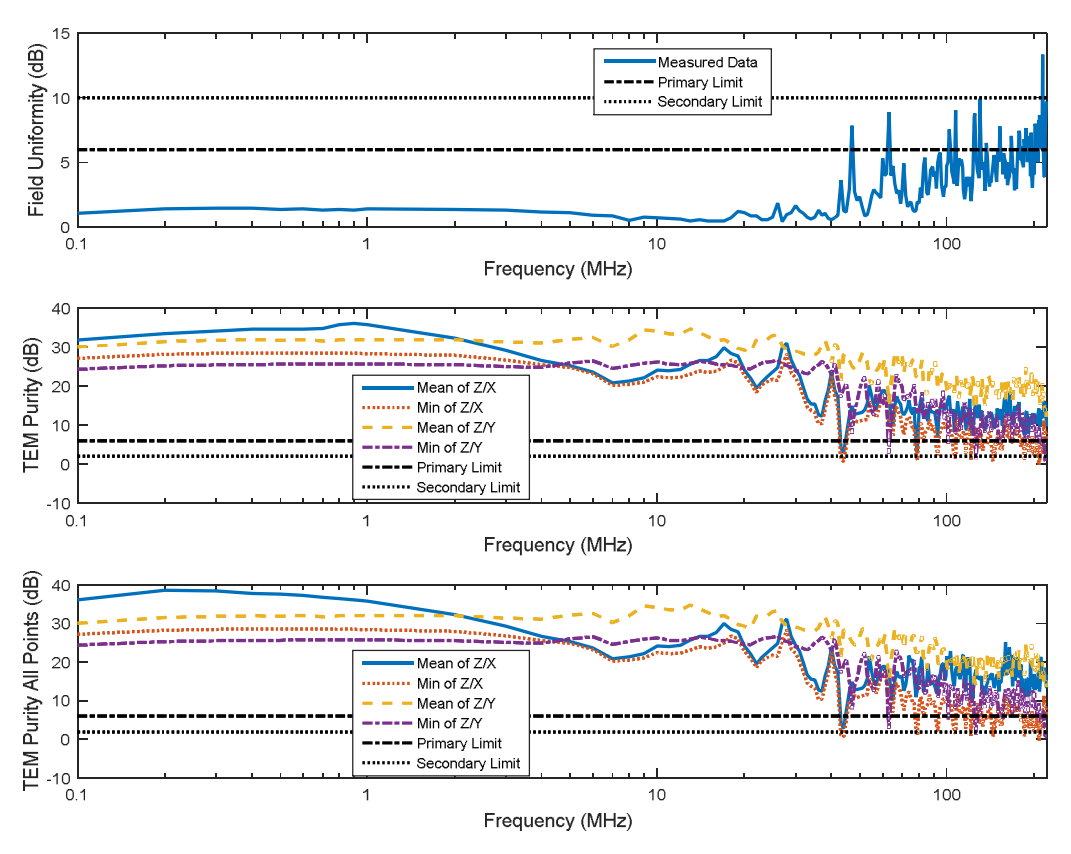


Figure 14. Radial Plane = 1, 2 m x 2 m area
Uniformity Specification < 6 dB; Purity Specification > 6 dB

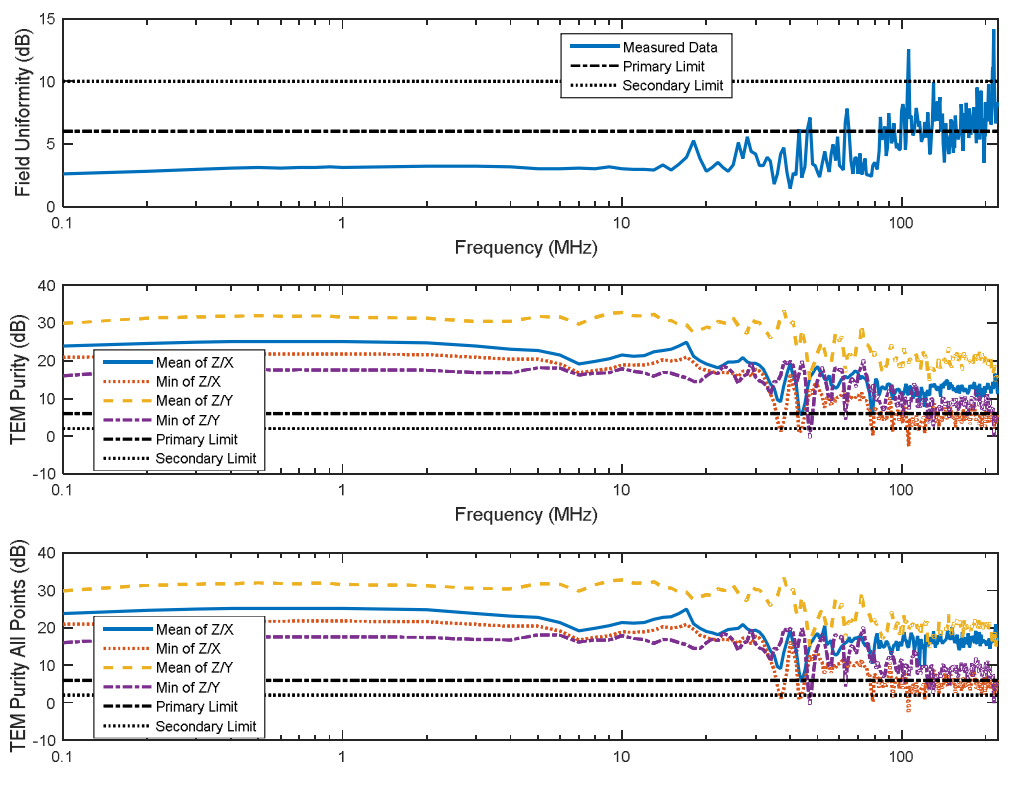


Figure 15. Radial Plane = 2
Uniformity Specification < 6 dB; Purity Specification > 6 dB

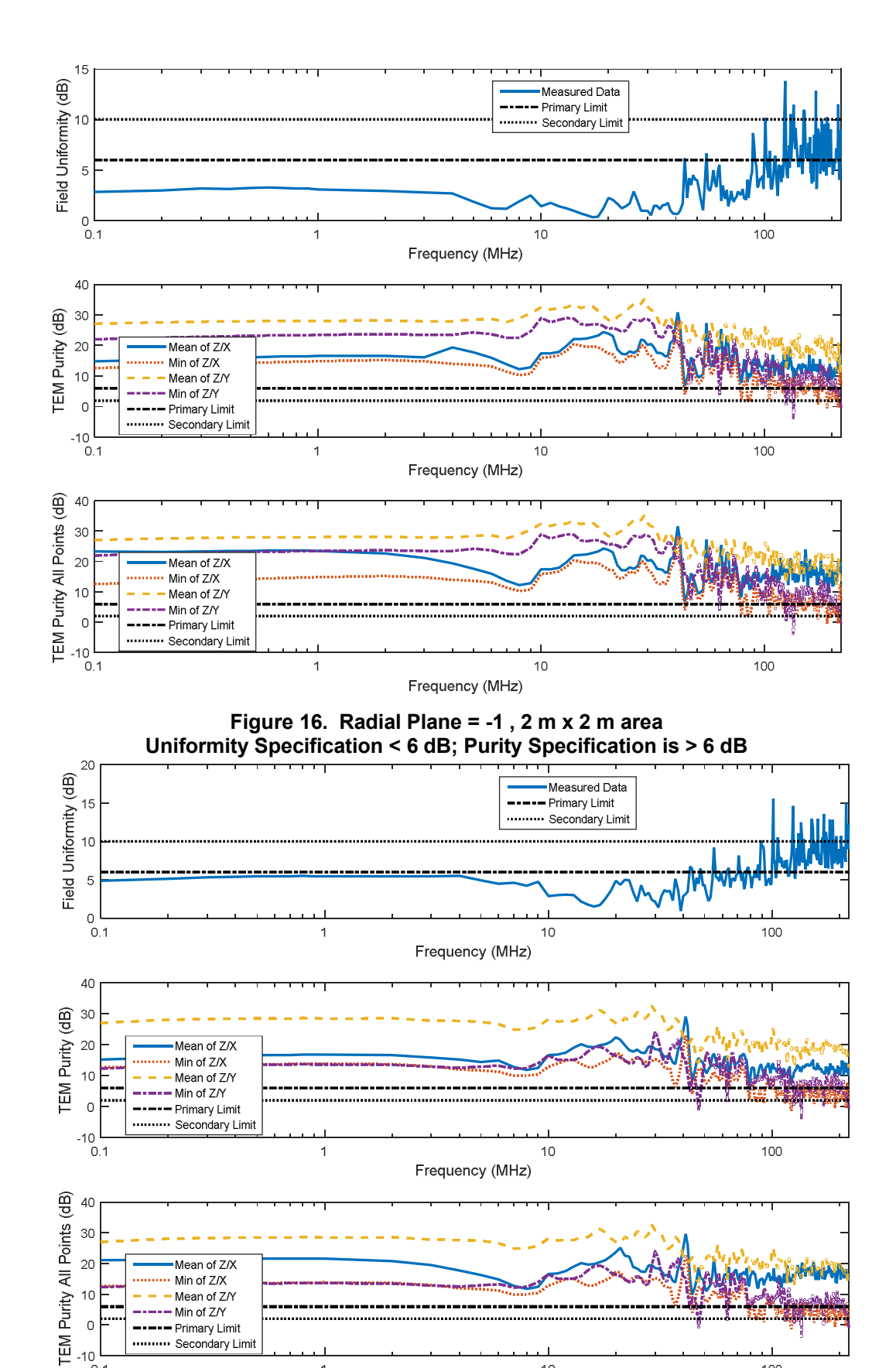


Figure 17. Radial Plane = -1
Uniformity Specification < 6 dB; Purity Specification > 6 dB

Frequency (MHz)

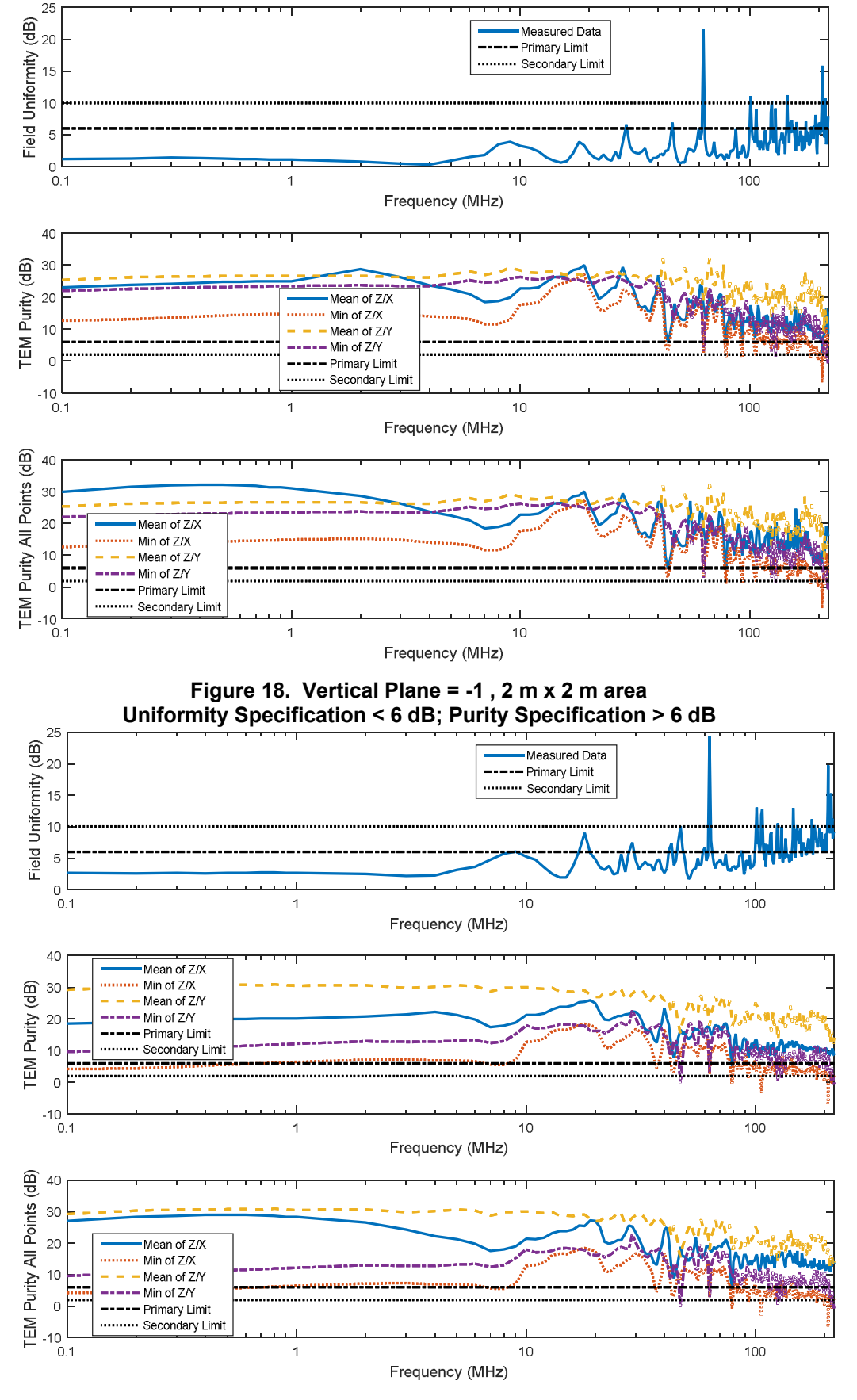


Figure 19. Vertical Plane = 1
Uniformity Specification < 6 dB; Purity Specification > 6 dB

The next group of figures shows E-field strengths in planes normal to the desired direction of propagation. Figure 20 shows 200 kHz measurement results. The complete data set contains results between 100 kHz and 220 MHz. The top row represents the mean of all reference probe data taken for this plane and serves as a reference for the reader. The red dot in each graph indicates the frequency of data shown in the lower graphs.

The lower three graphs are a representation of each electric field component in the plane. Each line represents the E-fields at heights of -1, 0, and 1 m in EMES (see Figure 2). The dot-dash line shows a reference for the theoretical normalized electric field. It is clear that the center graph, representing the vertical component, is significantly higher in amplitude and uniformity than the radial and horizontal components and is very close in magnitude to the theoretical value. The radial and horizontal components are at least 10 dB below the primary field. The shape of the normalized E-field plot shown in the center plot is as expected from theory described in reference (Crawford, Generation of Standard EM Fields Using TEM Transmission Cells, November 1974).

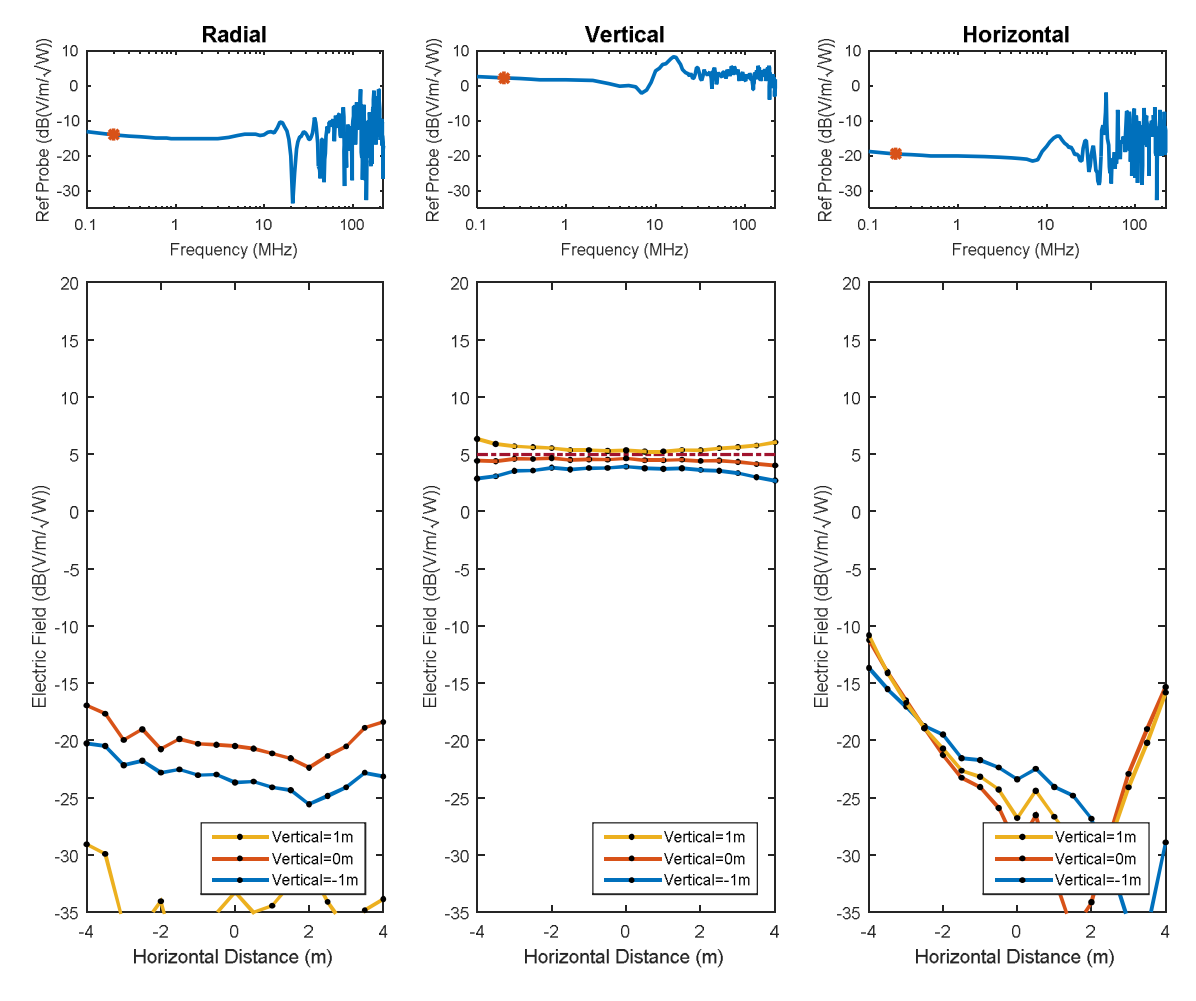


Figure 20. 200 kHz Results, Radial = 0 m Plane

Figure 21 shows the same result shown in Figure 20 at 8 MHz. At this frequency, the amplitude is the minimum value measured for all frequencies. Reflection from the termination causes the magnitude of the electric field to drop almost 5 dB. At this frequency the dominate reflection is from the cones and back wall and any reflections from side structures are minimal. Again, the dot-dash line in the plot shows the theoretical value without contribution from reflections. The radial and horizontal components are 15 dB lower than the primary field.

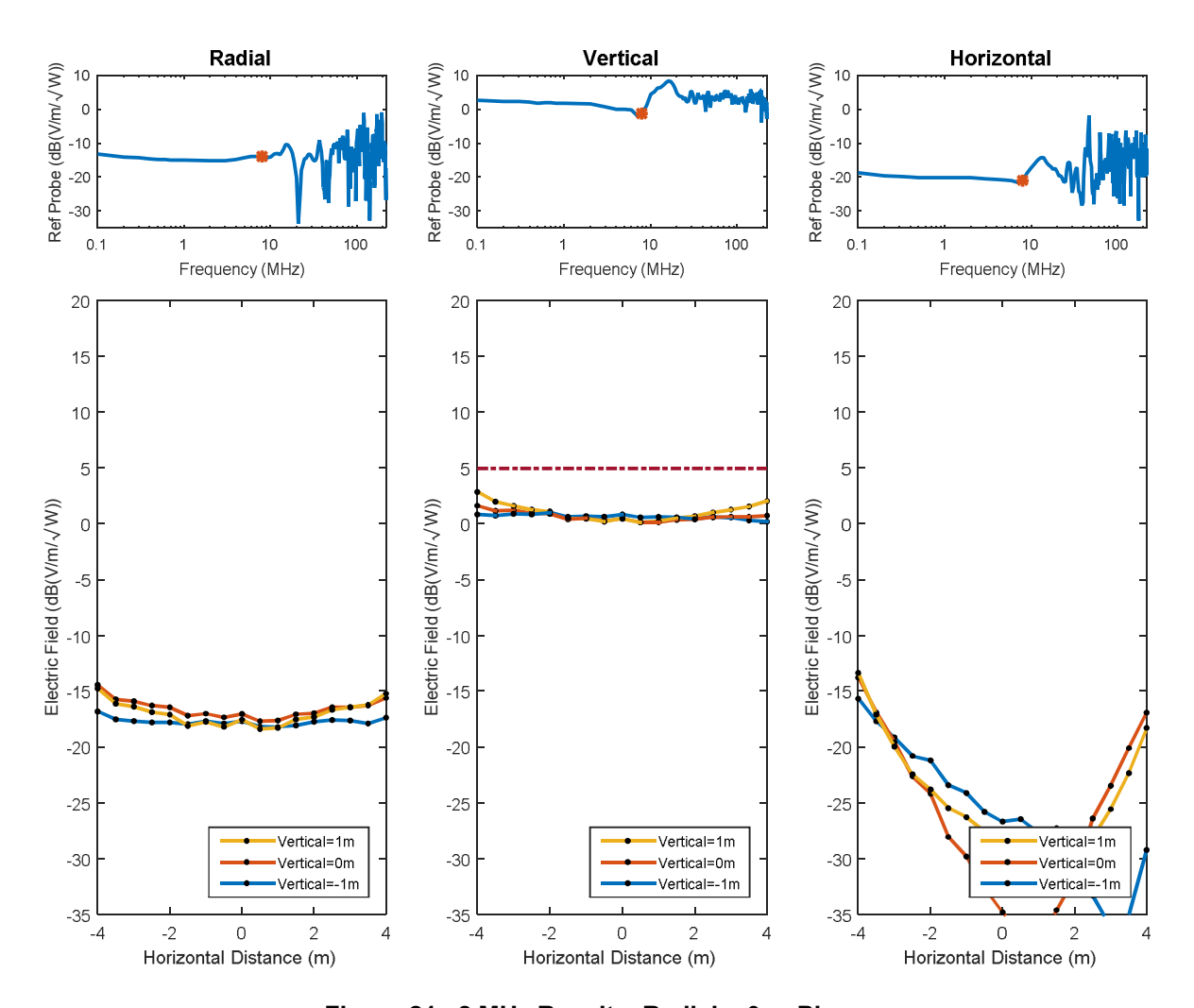


Figure 21. 8 MHz Results, Radial = 0 m Plane

Figure 22 shows results for 15 MHz. At this frequency, the vertical field is at its maximum. This is a consequence of reflections from the termination and back wall. The radial and horizontal components are about 10 dB less than the primary field. The dominant field strength is about 3 dB above the expected value marked on the graph by the dot-dash line. The return loss is -7.7 dB or a VSWR = 2.4. At the terminals to EMES, the measured VSWR is 3.1 at 10 MHz. These results suggest that more than EMES termination contribute to the return loss and VSWR seen at EMES input. The connector at the feed contributes the total VSWR into EMES.

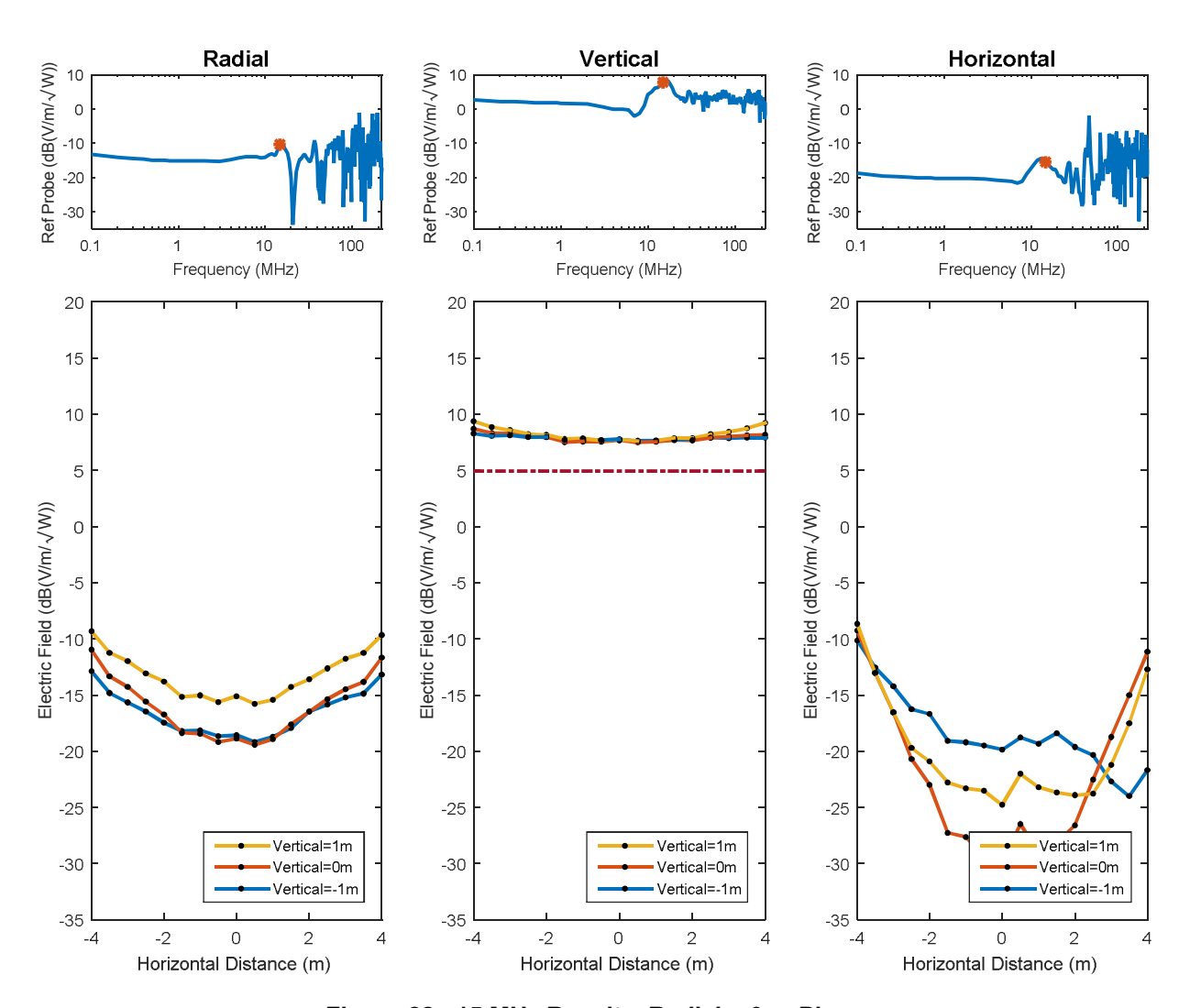


Figure 22. 15 MHz Results, Radial = 0 m Plane

Figure 23 shows results for 47 MHz. Cross polarized values exceed the primary values in a number of locations for a number of frequencies. This is one example where cross polarization components are significant contributors to the total electric field strength, with the horizontal component at 2 and -2 meters from the center higher in amplitude than the values for the vertical component.

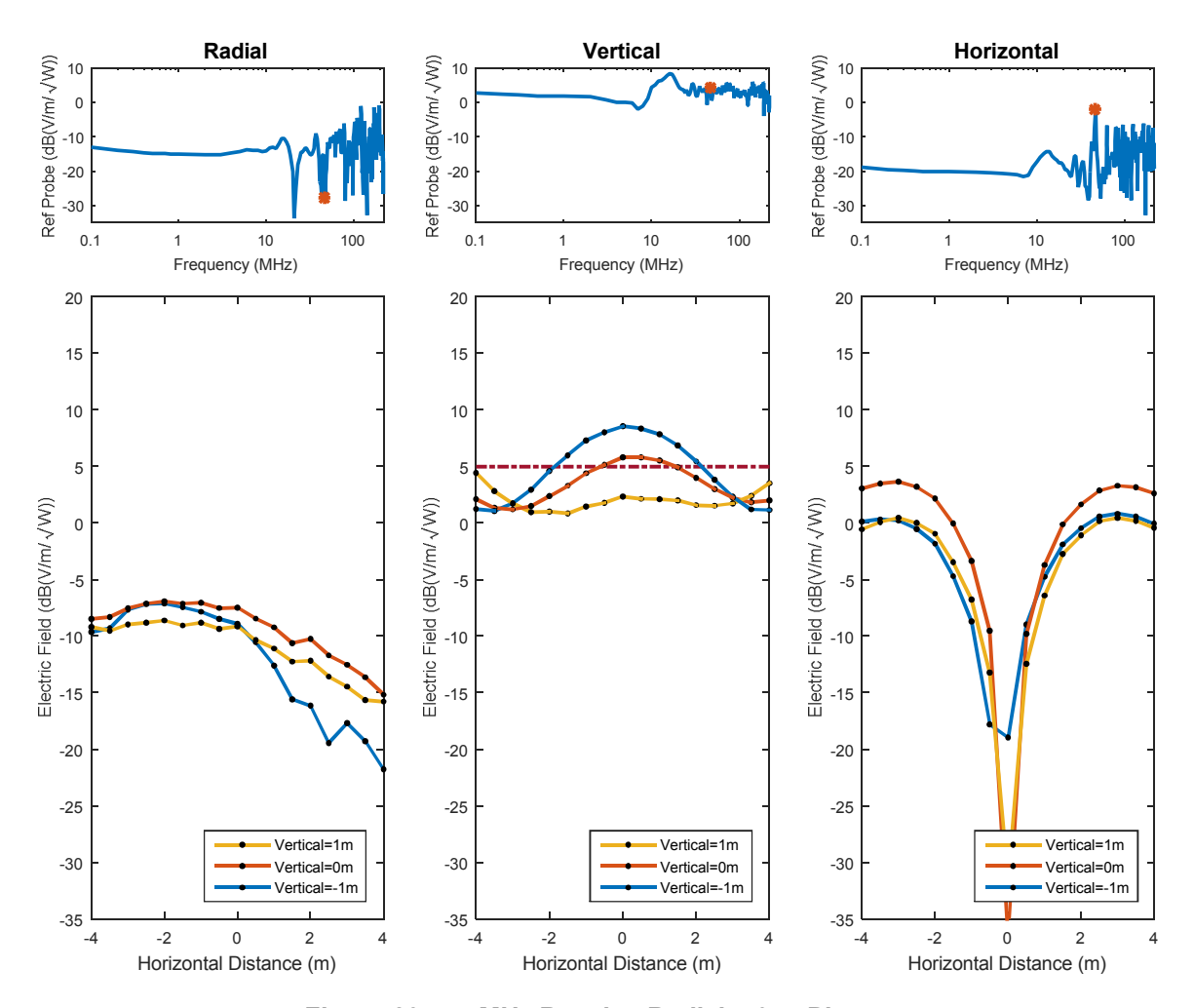


Figure 23. 47 MHz Results, Radial = 0 m Plane

Figure 24 shows 63 MHz results. It is clear from the center graph that the field is no longer uniform by most definitions. The cross polarization values are elevated indicating that EMES is behaving more as a cavity than a transmission line. The vertical component measured by the ETS probes does not discriminate the different modes that contribute to the total field; all reflections contribute to the measured electric field. For 63 MHz, the horizontal and radial responses suggest that the reflections off the wall are symmetric. Not all results from other frequencies exhibit this symmetry.

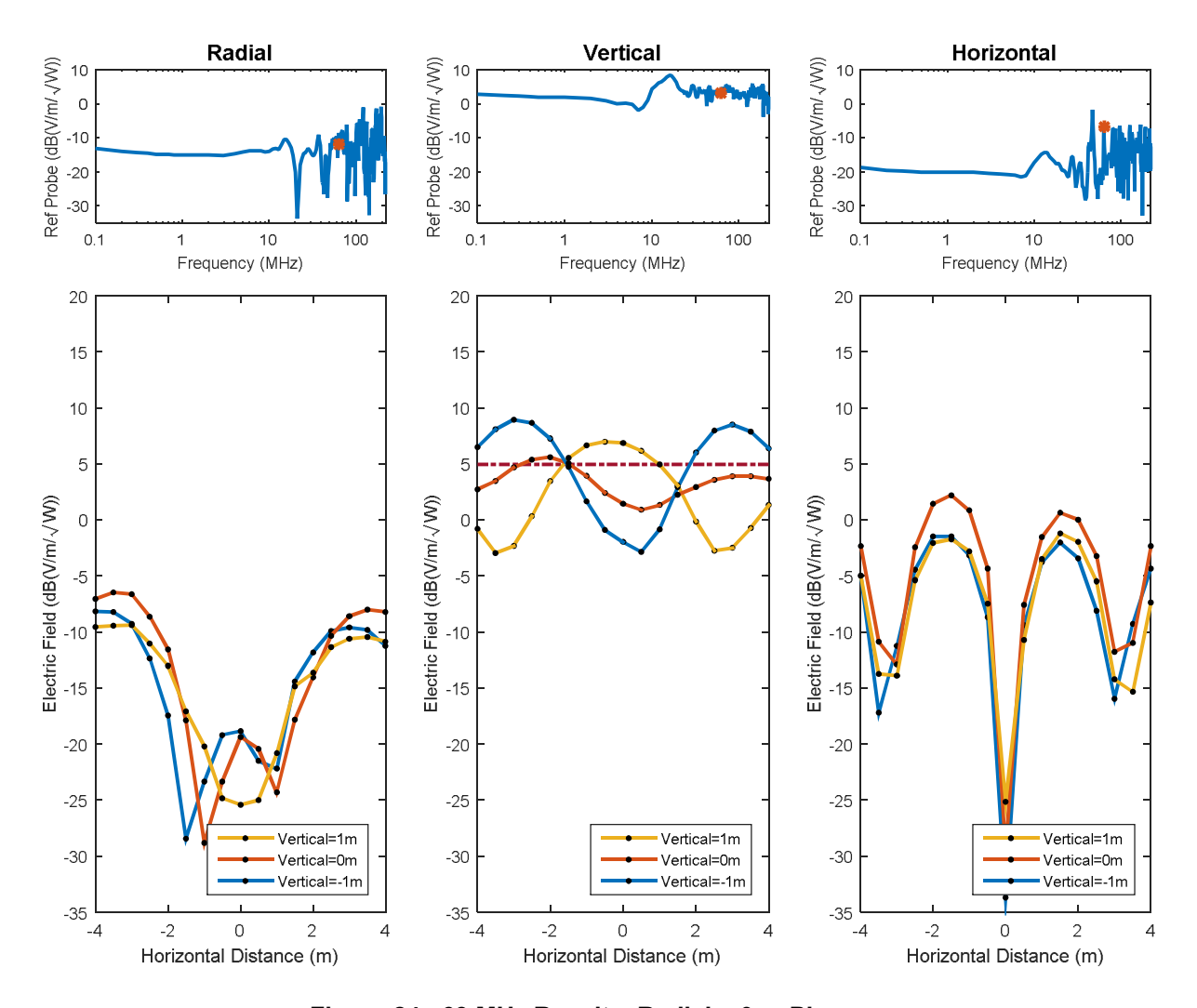


Figure 24. 63 MHz Results, Radial = 0 m Plane

Figure 25 through Figure 29 show EMES response over the Horizontal = 0 plane. Figure 25 shows E-fields are more uniform at the front of EMES than near the absorbers. Recall that the -2 m is nearest the cones. Cross polarized components, especially the radial component, have significant amplitude compared to the vertical in the aft part of EMES; so cross polarized components contribute much less to the total field at the front end of EMES working area than the end near end.

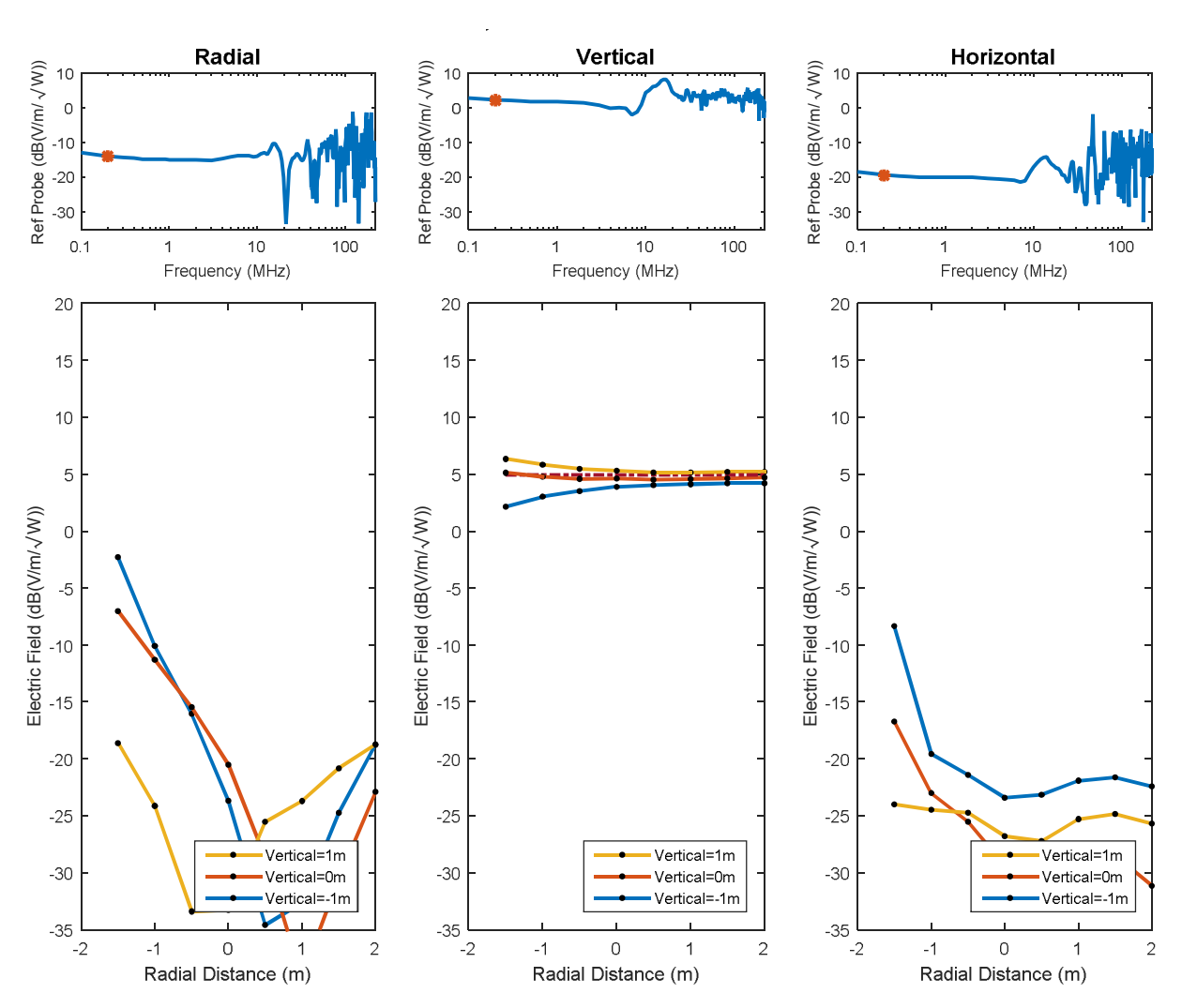


Figure 25. 0.2 MHz Results, Horizontal = 0 m Plane

Figure 26 shows a 6 dB drop in field strength between EMES front and aft regions at 8 MHz. The cross polarization components also increase towards the aft end of EMES.

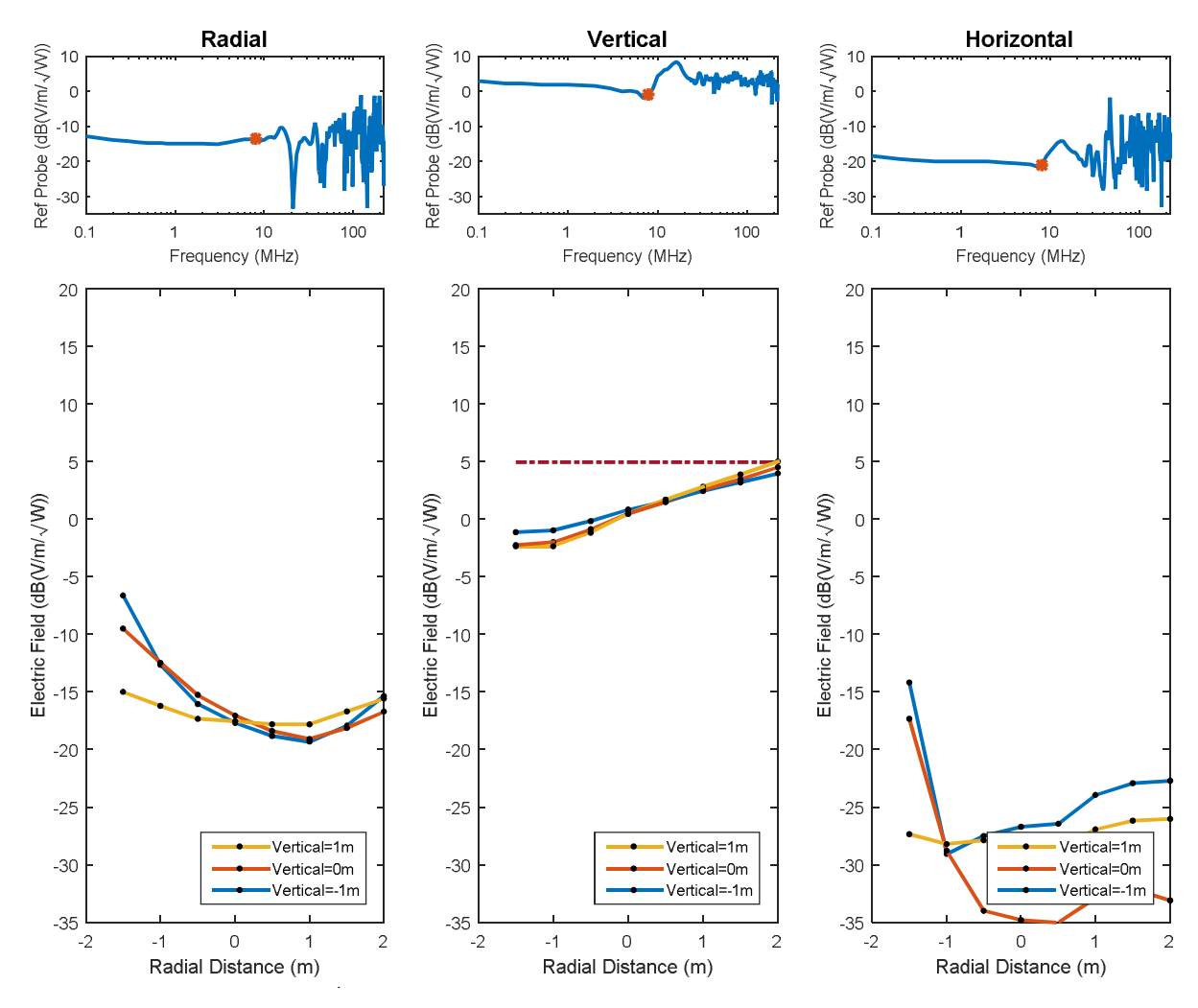


Figure 26. 8 MHz Results, Horizontal = 0 m Plane

Figure 27 shows that the fields increase above the expected values at 15 MHz. This result is consistent with the E-field at Radial = 0 results presented earlier in this report. The cross polarization components are significantly less than the vertical component. This result is consistent with EMES input having the highest reflection coefficient in the radial = 0 plane as shown in Figure 8.

Combined results in Figure 22 and Figure 27 clearly show a geometric saddle surface. Both figures also indicate that the E-field does not significantly change from top to bottom.

Figure 23 and Figure 28 both show a clear increase in the field strength at heights of -1 m and 0 m in the center of EMES while the field does not fluctuate as much for a height of 1 m.

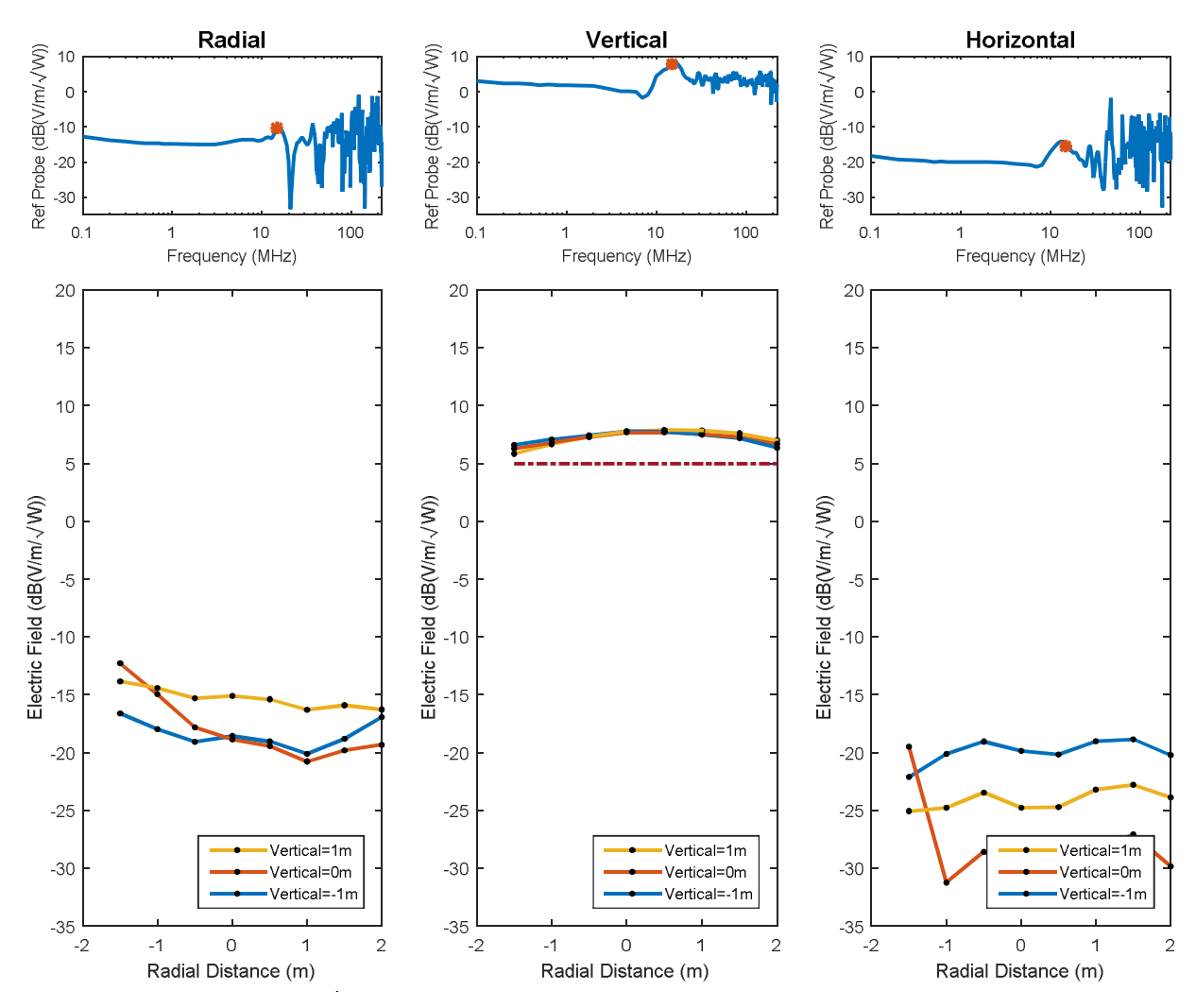


Figure 27. 15 MHz Results, Horizontal = 0 m Plane

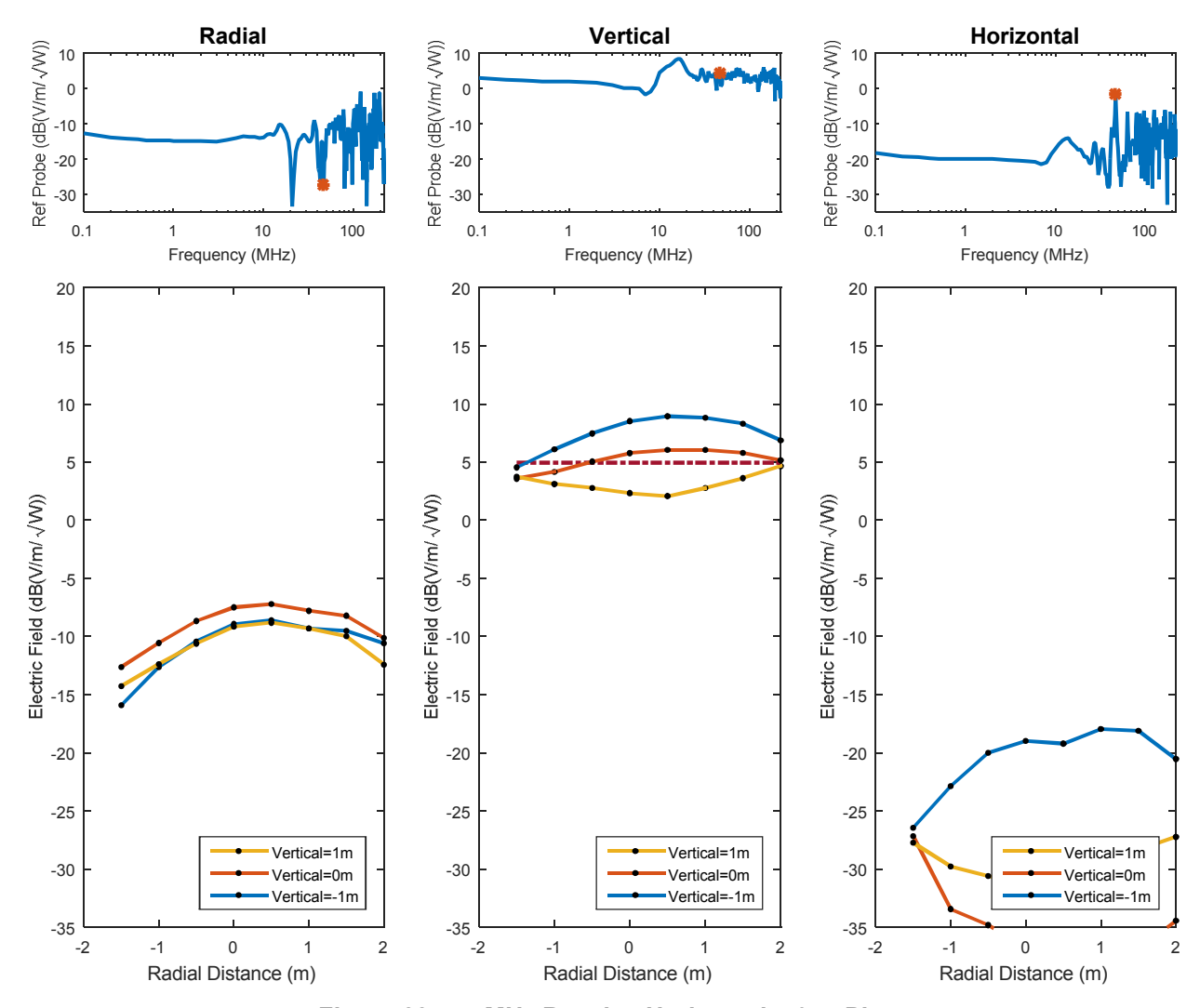


Figure 28. 47 MHz Results, Horizontal = 0 m Plane

Figure 24 showing the radial = 0 plane and Figure 29 showing the horizontal = 0 plane indicate that EMES exhibits a strong resonance effect at 63 MHz. The -1 m vertical height drops 28 dB from the front and aft to the center. In the center of Figure 29, the field strength drops 18 dB in $\frac{1}{2}$ meter. 63 MHz is the frequency where EMES exhibits the strongest field strength variation.

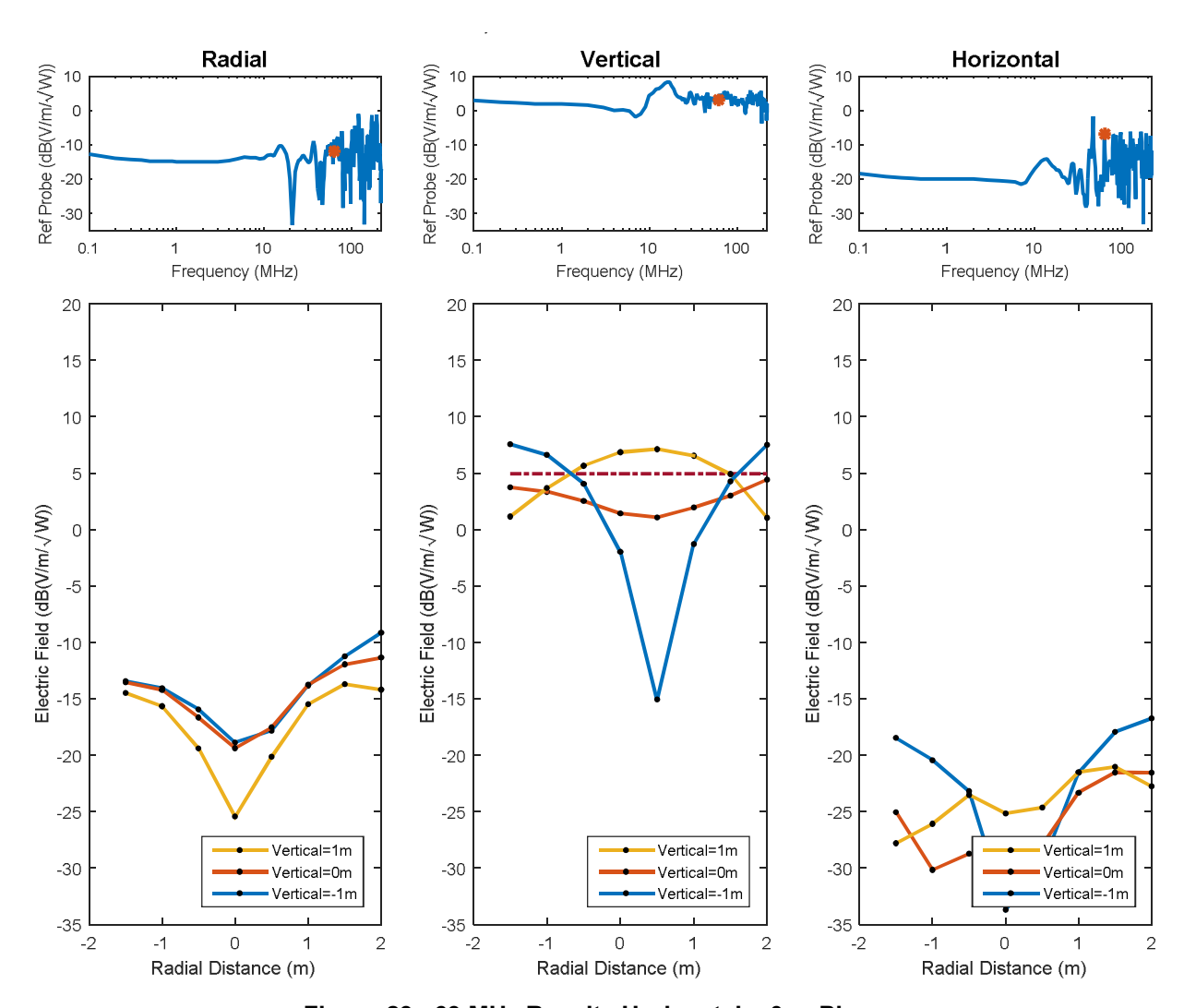


Figure 29. 63 MHz Results Horizontal = 0 m Plane

In addition to the electric field measurements, we measured the magnetic field along the center of EMES (radial = 0). Figure 30 shows results of magnetic field measurements at vertical = 0 and radial = 0 and compares these results to electric field measurements on the same line. The results shown are the H-field measurements converted to its free field E-Field equivalents and the E-field measurements. The conversion makes the comparison easier to interpret. H-field data exist for the full frequencies range of this study. At 0.2 MHz comparison between the E-field results and the H-field results show good agreement. Further, both also agree with the theoretical

value of about
$$5^{\left(\frac{V}{m}\right)} / \sqrt{watt}$$

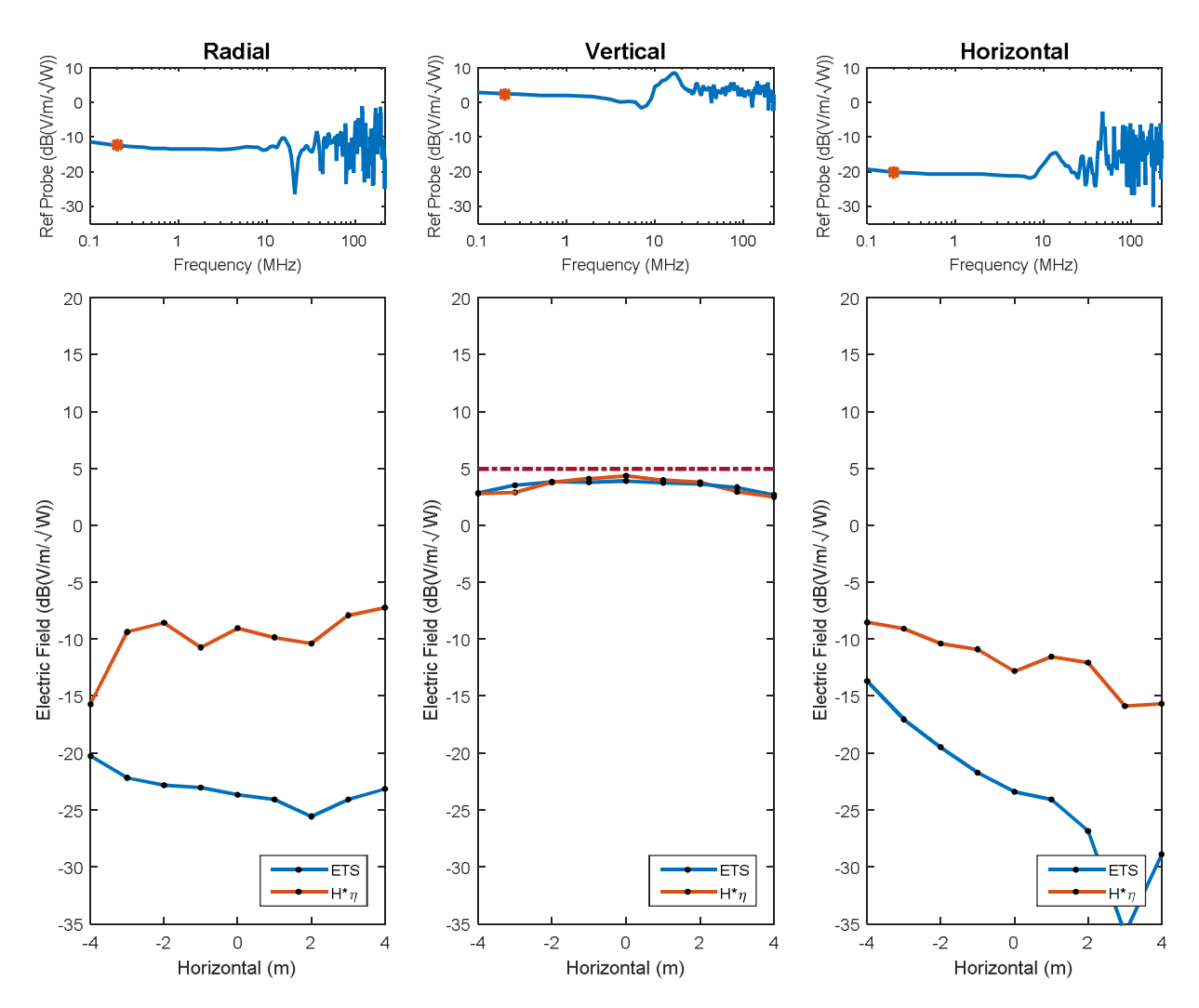


Figure 30. H-field Measurement at 0.2 MHz

Figure 31 shows H-field results at 7 MHz. Each probe, whether magnetic or electric, reads a vector sum of magnetic or electric field from the combination of the incident wave and any reflected waves generated in EMES. Reflection from the back wall strengthens the magnetic field and weakens the E-field at 7 MHz. At the center of EMES, the magnitude of the magnetic field increase is the same as the electric field reduction: about 4.5 dB. The vertical component measured at any point is the sum of components from the feed, the sidewalls, and the back wall. The magnetic fields from these contributions are not likely to align the same as for the electric field. In fact, they most likely will not align. Results for the 7 MHz case clearly show the electric and the equivalent magnetic field do not agree with each other or with the expected field strength based on the design and geometry of EMES. Therefore caution should be used if electric fields are going to be based on magnetic field measurements.

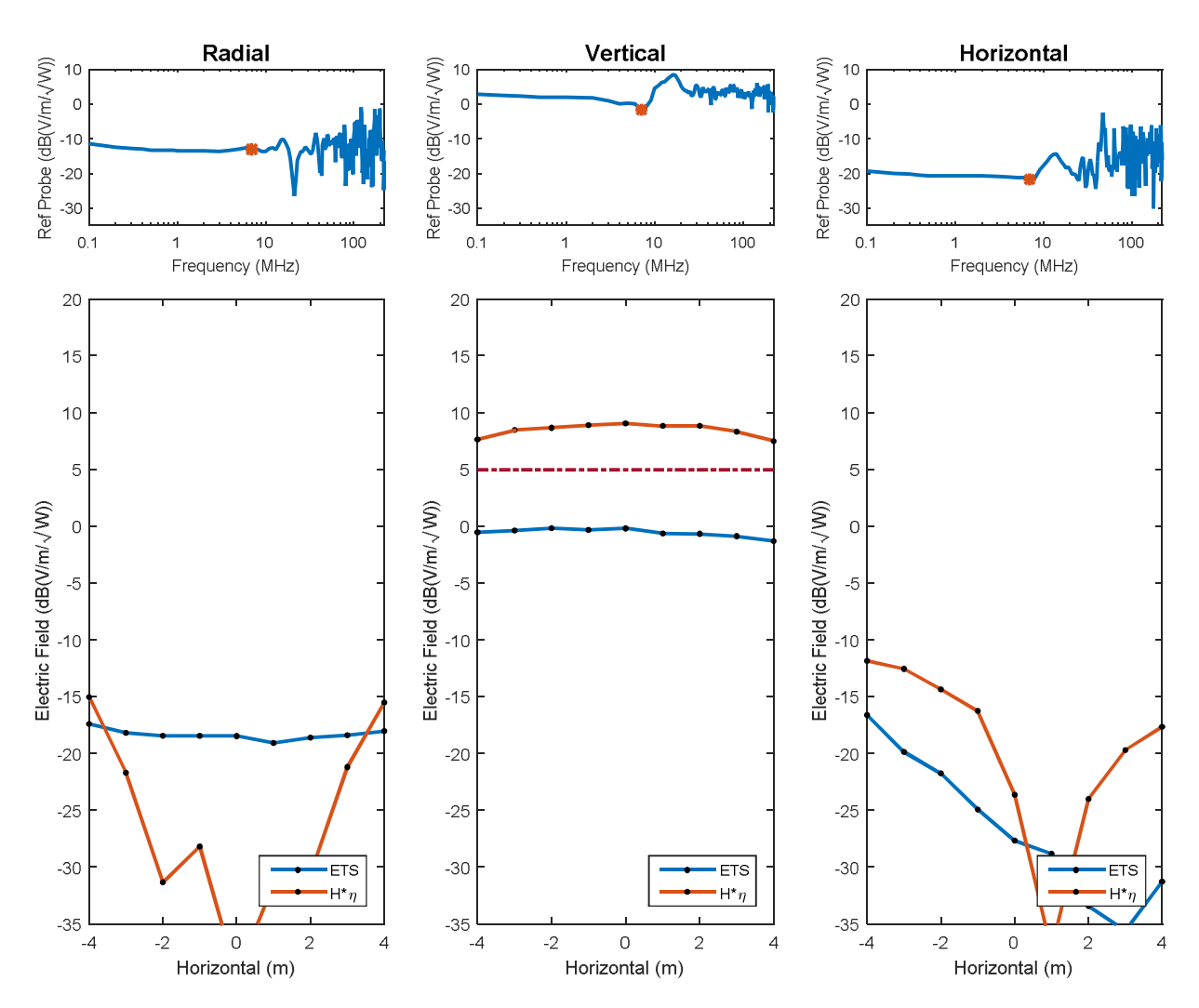


Figure 31. H-field Measurement at 7 MHz

Figure 32 also shows a disagreement between the E and H fields as discussed above. The frequency where the E-field was at a true minimum is likely between 7 and 8 MHz, while the magnetic field is at a maximum for the same frequency. As seen in the reference plots at the top and a comparison of Figure 31 and Figure 32, it is clear that the behavior of EMES changes slowly in this frequency range.

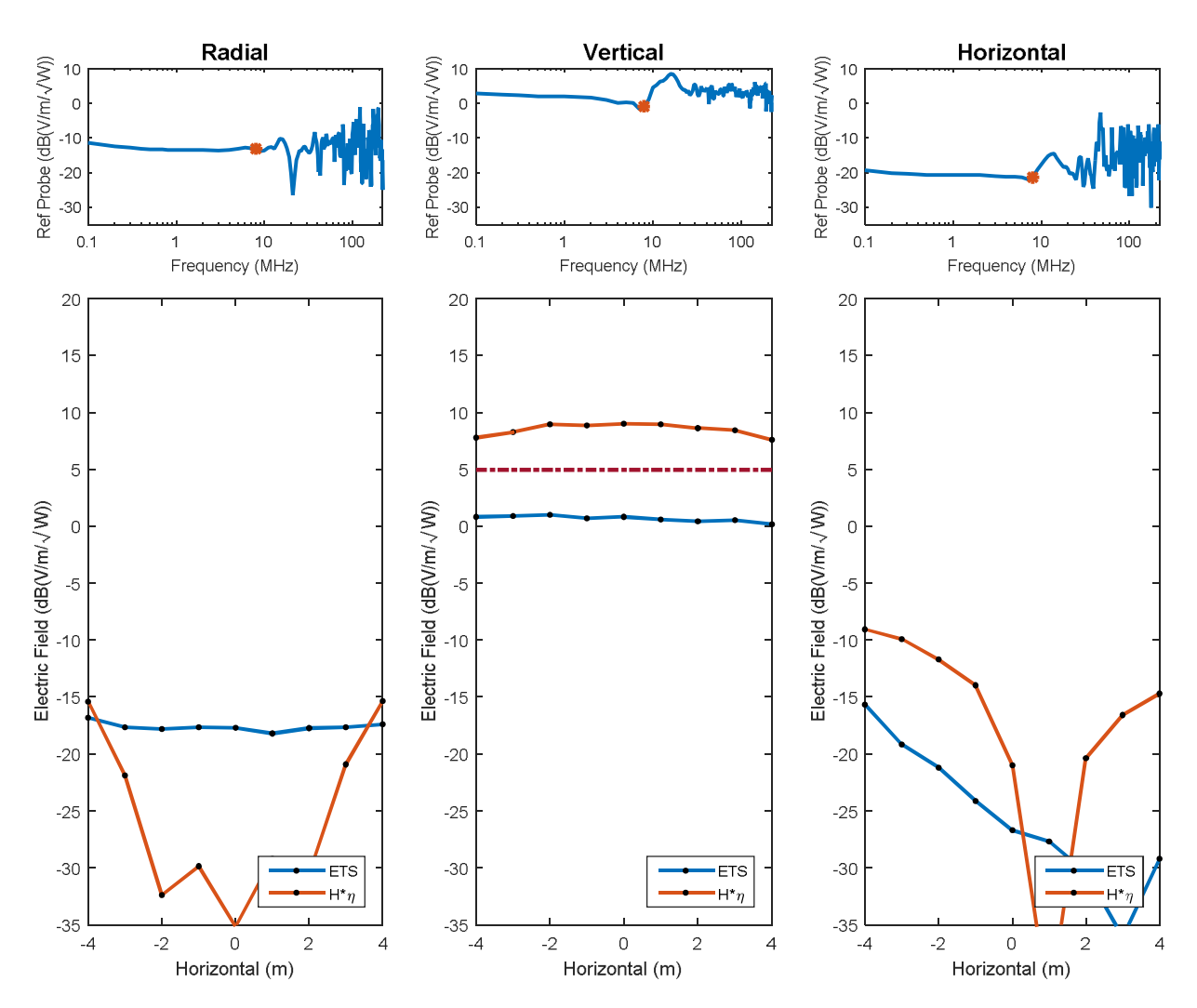


Figure 32. H-field Measurement at 8 MHz

This result is a consequence of the reflected wave traveling in the opposite direction from the incident wave. Using Poynting equation, $S = E \otimes H$, we see which direction the energy must propagate. The EM field reflected and incident waves will add as vectors. Figure 33 illustrates the relationship between reflected H-field and E-field. The reflection from the back wall reduces the E-field while the H-increases. In addition

Figure 34 shows 15 MHz results. In this case, the total E-field is at a maximum and the H- field is at a minimum. The 15 MHz results are different from at 8 MHz because the higher frequency has a shorter wavelength, hence the reflected energy is $\frac{\pi}{2}$ out of phase in the 15 MHz case compared to 8 MHz. Measurements occurred in 1 MHz increments, therefore the two frequencies are most likely not exactly even multiples apart.

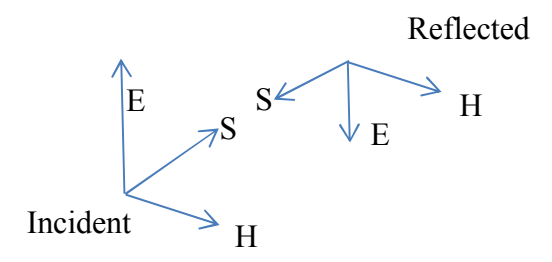


Figure 33. Direction of Propagation

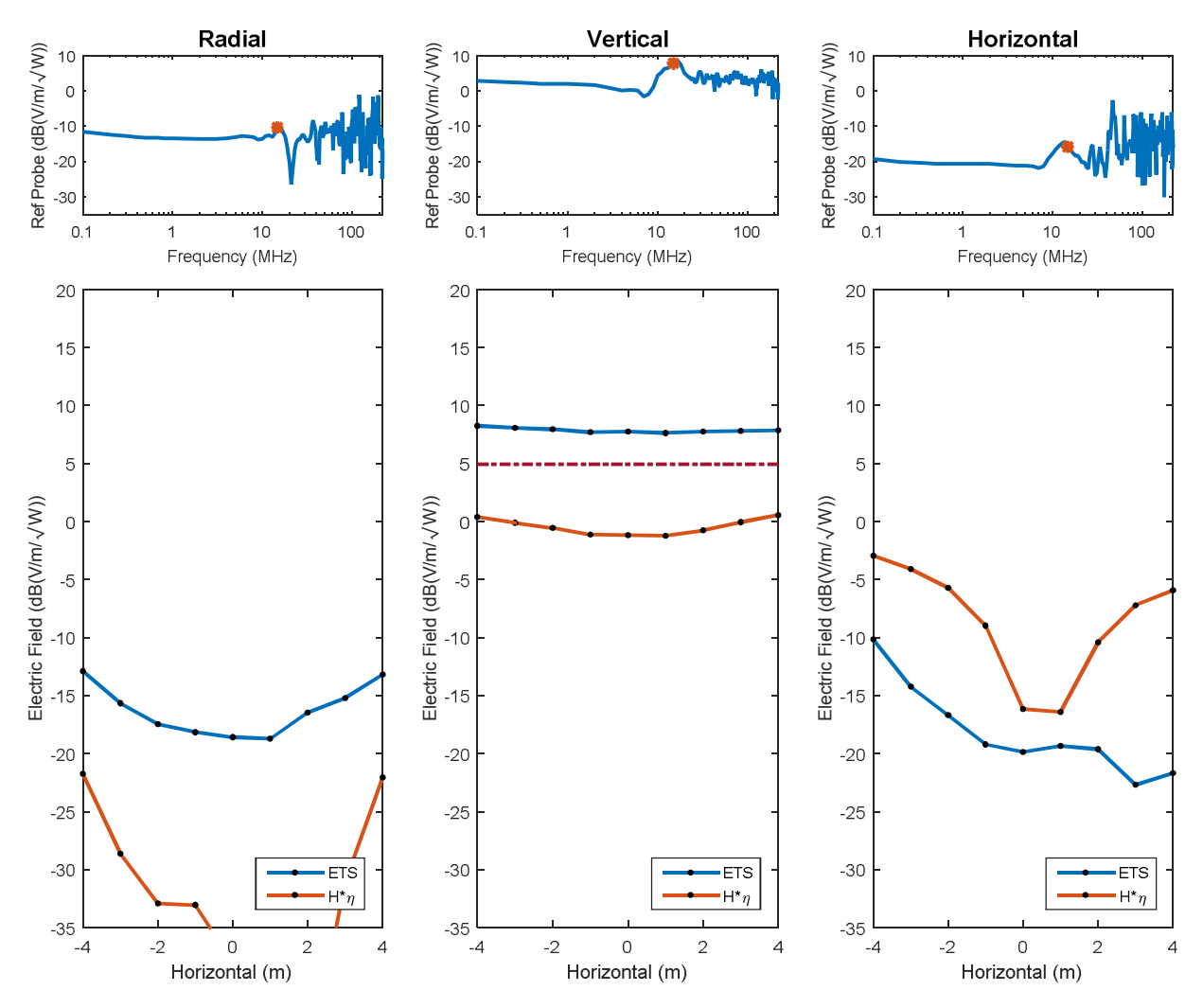


Figure 34. H-field Measurement at 15 MHz

Figure 35 shows H-field measurement results at 47 MHz (about the 6th harmonic of 8 MHz). Comparing these results to the 8 MHz case shows a significant increase in the horizontal component, 20 dB greater at 47 MHz than at 8 MHz.

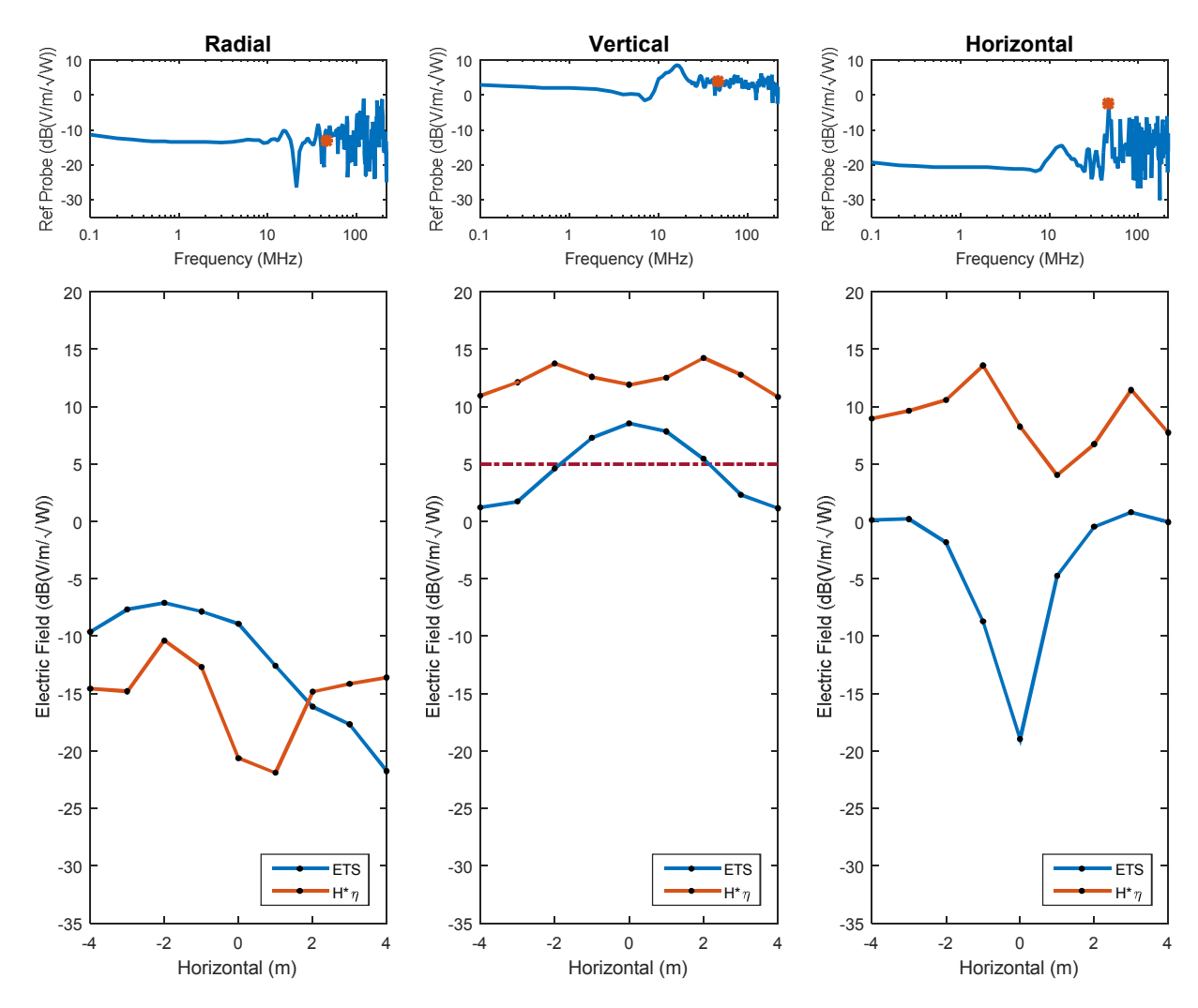


Figure 35. H-field Measurement at 47 MHz

Figure 36 shows the 63 MHz result. This result is roughly the 8th harmonic of the 8 MHz measurement. In this case, the E- field for the three different heights seen in Figure 29 varies significantly; however, all clearly show a cavity effect. Measurement of the H-field at a single frequency shows a similar cavity effect. H-field follow the same response as the E-field. The agreement between the two is not always as shown here.

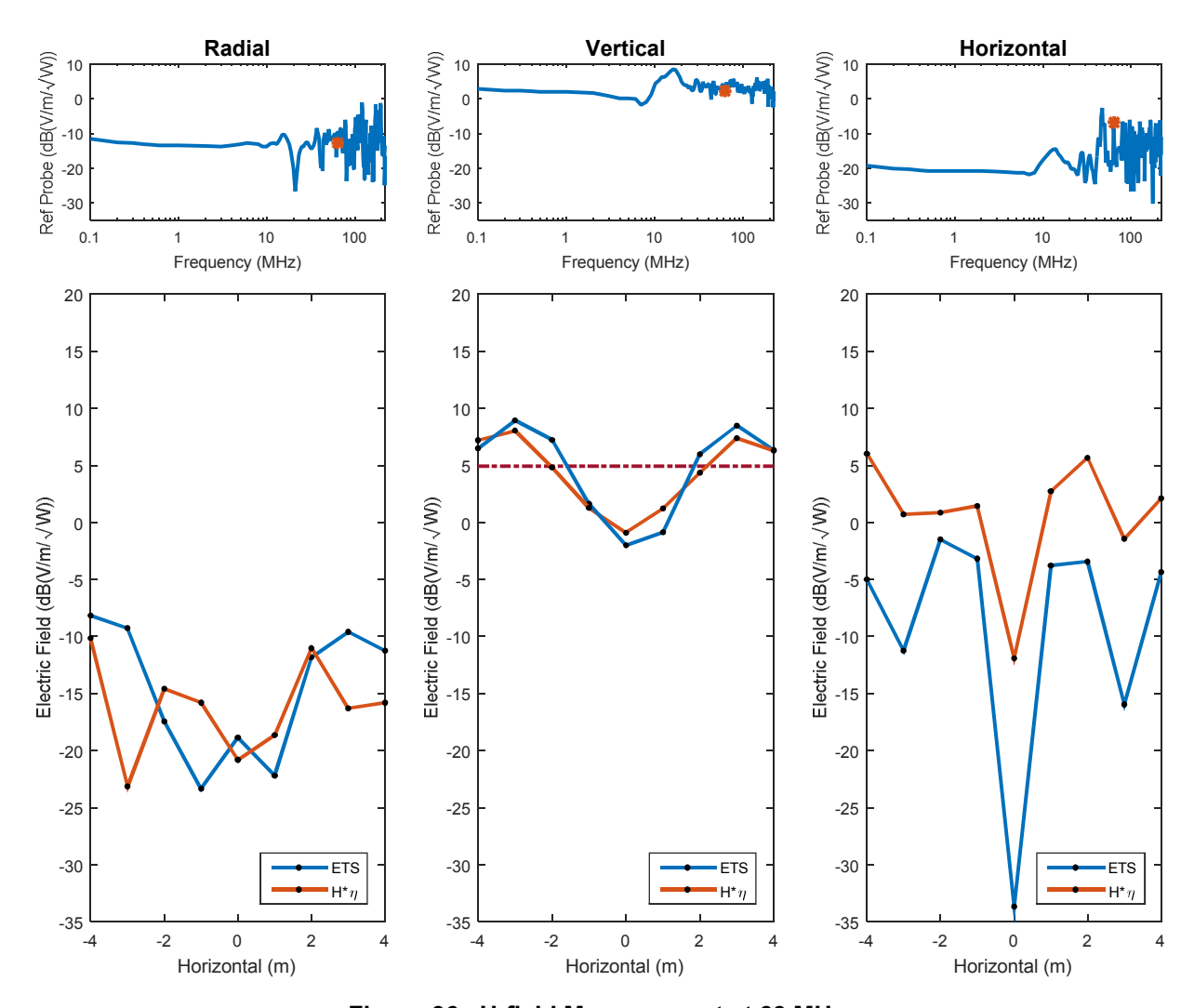


Figure 36. H-field Measurement at 63 MHz

6. RECOMMENDED APPLICATION OF THIS DATA

The purpose of this study was to characterize and record the performance of the EMES for use by NW qualification programs. RPSS requires knowledge of the uncertainty of any measurement used to evaluate the qualification of a NW system, subsystems, and components. To meet this requirement, this report contains information used to estimate field strength variation over the area that a test object would occupy. The known variation in field strength is then part of the assessment to quantify the uncertainty of a measurement conducted in EMES.

In this report, we provide a sample result for two areas: 8 m x 2 m and 2 m x 2 m. Department 1353 retains the measurement results so that they are available to compute the field variation over any volume required by a specific test program. IEC 61000-4-20 (Testing and measurement techniques – Emission and immunity testing in transverse electromagnetic (TEM) waveguides) provides the foundation for the evaluation in this paper.

To apply information in this report to a test program, one uses the purity and uniformity plots. Both plots provided a measure of EMES performance.

A uniformity analysis using the data obtained in this effort and the specific area matching the size of a test object will provide the information needed for an uncertainty analysis. It should be noted that test objects placed in this facility will have an effect on the field structure. The size of the object and materials that it is created from will determine the significance of that impact.

7. REFERENCES

- Caldwell, M., & Higgins, M. (2005). Electromagnetic Test Facilities at Sandia National Laboratories. *Proceedings of the IEEE Instrumentation and Measurement Technology Conference, IMTC 2005.*, 1.
- Crawford, M. L. (November 1974). Generation of Standard EM Fields Using TEM Transmission Cells. *IEEE Transactions on Electromagnetic Compatibility, EMC-16*(4).
- Crawford, M. L., & Workman, J. L. (July 1981). Using a TEM cell for EMC measurements of electronic equipment. *NBS Tech Note* 1013.
- Malaric, K., Bartolic, J., & Modlic, B. (2000). Absorber and resistor contribution in the GTEM-cell . *IEEE International Symposium on Electromagnetic Compatibility*, *2*, 891-896.
- Pollard, N. (1977). *Broadband Electromagnetic Environments Simulator (EMES)*. Albuquerque, NM: SAND-77-0039c, CONF-770806-1, Sandia National Laboratories.
- Reed, J. O. (July 1974). EMR/EMP Parallel Plate Transmission Line Facility.
- Salazar, R. A. (January 2016). EMES Capability.
- Seely, G. A., & Thomas, W. R. (1978). *Low Frequency Performance of the EMES Facility*. Performed under contract 07-9955 by Science Applications Incorporated.
- Varnado, G. B. (1975, SAND1975-0412). *The Electromagnetic Environments Simulator (EMES)*. Albuquerque, NM: Sandia National Laboratories.

DISTRIBUTION

1	MS0899	Technical Library	9536 (electronic copy)
10	MS1152	Robert Salazer	Org. 1353
1	MS1152	Robert Salazar	Org. 1353(electronic copy)
1	MS1152	Steven Glover	Org. 1353(electronic copy)

